AIAA JOURNAL
Vol. 48, No. 5, May 2010

Sound Transmission from a Source Outside a Nonisothermal Boundary Layer

L. M. B. C. Campos*
Instituto Superior Técnico, 1049-001 Lisbon Portugal
and
M. H. Kobayashi†
University of Hawaii at Manoa, Honolulu, Hawaii 96822

DOI: 10.2514/1.40674

The transmission of sound from a source outside a nonisothermal high-speed boundary layer is considered. The sound source is assumed to lie in a uniform stream and matched to a zero velocity at the wall by a linear velocity profile. The unidirectional shear mean flow is assumed to be isentropic but nonhomentropic, so that the entropy, the sound speed, and the temperature can vary from one streamline to the other. The condition of homoenergetic flow, or constant enthalpy, is used to relate the sound speed to the mean flow velocity and specify the temperature profile in the boundary layer. Compared with a homentropic boundary layer, for which sound refraction is due to the shear flow alone, a nonhomentropic boundary layer introduces additional refraction due to the nonuniform sound speed and the associated temperature gradients. It is shown that for a high speed, even in isentropic conditions, the nonhomentropic effects of temperature gradients and the nonuniform sound speed can cause significant sound attenuation (viz., for the same sound source outside the boundary layer, the acoustic pressure at the wall can be substantially reduced). This agrees qualitatively with the results from testing propfans at high subsonic speeds, which showed significant sound attenuation in the fuselage boundary layer.

Nomenclature

$A, B, C, D,$ E, F, G, H	=	constants in extended Heun equation (A5) [also F in Eq. (23b)]
a_n	=	coefficients [Eq. (31)] in series expansion [Eq. (28)].
b	=	stagnation enthalpy [Eq. (A2)]
b_n	=	coefficients [Eq. (32)] in series expansion [Eq. (30)]
c, c_o, c_∞	=	sound speed [Eq. (4a)], stagnation value [Eq. (11a)], and value in freestream [Eq. (38a)]
e	=	density of internal energy [Eq. (A1)]
e_n	=	coefficients [Eq. (B7)] in series expansion [Eq. (B6)]
h	=	enthalpy [Eq. (A1)]
I	=	dependent variable [Eq. (25b)] in differential equation (26)
J	=	dependent variable [Eq. (19b)] in differential equation (20)]
K	=	transverse wave number in freestream [Eq. (35)]
$\bar{K}$	=	integration variable [Eq. (C1)]
k	=	longitudinal wave number [Eq. (7)]
L	=	boundary-layer thickness [Eq. (33)]
M_∞	=	Mach number of freestream [Eq. (38b)]
N	=	number of degrees of freedom of a molecule of gas [Eq. (12a)]
$P(y; k, \omega)$, $P_\infty(y; k, \omega)$	=	acoustic pressure spectrum for wave of frequency ω and longitudinal wave number k at a distance y from the wall inside [Eq. (7)] and outside [Eq. (34)] the boundary layer
$p(x, y, t)$	=	acoustic pressure perturbation [Eq. (3)]
p_o	=	mean flow pressure [Eq. (2b)]
$Q, Q_1,$ Q_2, Q_{22}	=	solution of wave equation (27b) of first [Eq. (28)], second [Eq. (29)] kind, and complementary function [Eq. (30)]
R	=	dependent variable in acoustic-wave equation (24), as a particular case of the generalized Heun equation (B1)
S	=	strength of sound source [Eq. (34)]
T, T_o	=	temperature and stagnation values [Eq. (11c)]
t	=	time [Eq. (1a)]
$U(y), U_\infty$	=	mean flow velocity [Eq. (1b)] in freestream [Eq. (33)]
x	=	longitudinal coordinate along wall [Eq. (1b)]
Y	=	dimensionless distance from critical layer [Eq. (27a)]
$y, y_c, y_\pm, y_o$	=	distance from wall [Eq. (1a)] of critical layer [Eq. (18a)], of critical flow points [Eq. (18b)], and of sound source [Eq. (34)]
z, z_c, z_+	=	distance from wall divided by boundary-layer thickness [Eq. (39a)] for critical layer [Eq. (39b)] and for upper critical flow point [Eq. (40)]
α, α_∞	=	dimensionless frequency parameter [Eq. (21a)] in freestream [Eq. (37a)]
β, β_∞	=	dimensionless wave number parameter [Eq. (21b)] in freestream [Eq. (37b)]
γ	=	ratio of specific heats [Eq. (4a)]
δ	=	Dirac delta function [Eq. (34)]
ε	=	dimensionless compressibility parameter [Eq. (11b)]
$\zeta, \zeta_c, \zeta_\pm$	=	dimensionless distance from critical layer [Eq. (22a)] and of critical layer and critical flow points [Eq. (23b)]
η	=	independent variable [Eq. (25a)] in differential equation (26)
$\xi, \xi_c, \xi_\pm$	=	dimensionless distance from wall [Eq. (19a)] and of critical layer and critical flow points [Eq. (23a)]
ρ, ρ_o	=	total mass density [Eq. (2a)] of mean flow [Eq. (3)]

Received 29 August 2008; revision received 14 December 2009; accepted for publication 29 December 2009.

*Center for Aeronautical and Space Science and Technology, Aerospace Mechanics Section.

†Department of Mechanical Engineering. 2540 Dole Street, Holmes Hall 302.

σ = index [Eq. (31)]
σ_{ij} = viscous stresses [Eq. (A1)]
χ = thermal conductivity [Eq. (A1)]
Λ, Λ_∞ = dimensionless parameter [Eq. (21c)] in freestream [Eq. (37c)]

I. Introduction

THE propagation of sound in isothermal shear flows is specified by the homentropic form of the wave equation [1–9], and has been studied mostly by numerical and approximate analytical methods, with three motivations in mind: 1) propagation in ducts containing a shear flow, such as jet engine ducts [10–21], 2) effect of boundary layers on sound near a wall, such as the fuselage or cabin of an aircraft [22–26], and 3) effect of laminar shear layers on sound transmission (e.g., shear layers of a jet exhaust and wakes of control or high-lift devices [27–32]). The model of a shear layer as a laminar shear flow of finite width [33] is intermediate between a vortex sheet [27,31] as a discontinuity of the tangential velocity and an irregular shear layer [34–39], which may entrain turbulence [40–46]. The acoustic-wave equation in a laminar shear flow has a singularity in which the Doppler-shifted frequency vanishes; the latter is calculated from the flow velocity, the wave frequency, and the horizontal wave number. The singularity corresponds to the critical level, extensively studied for various types of waves (e.g., internal [47–49], inertial [50], nondissipative [51], and dissipative [38,52–54] acoustic gravity; instability [55,56]; and nondissipative [54,57–63] and dissipative [64–68] hydromagnetic). Critical levels have been considered in the acoustics of shear flows as turning points [20,29,30,69].

The propagation of sound in shear flows is relevant to aircraft engine ducts (inlets or nozzles), to jet exhausts and jet mixing, and to boundary layers. In the case of high-speed jets and engine exhausts, the shear flow is combined with temperature gradients, and both change the sound speed, causing refraction effects. The acoustic-wave equation in a unidirectional shear flow has been known for a long time [1–7] in the homentropic case, which implies an isothermal flow but does not restrict the Mach number. Exact solutions of this wave equation are obtained most readily in the case of the linear velocity profile using 1) parabolic cylinder functions [70], 2) Whittaker functions [33,71], 3) confluent hypergeometric functions [32,72,73], and 4) decomposition into functions (even and odd) relative to the critical layer [74]. The critical level corresponds to the vanishing of the Doppler shifted frequency and can lead to sound absorption. This has also been demonstrated for the exponential boundary layer [75] and the hyperbolic tangent shear layer [76] when the wave equation can be solved in terms of extended Gaussian hypergeometric functions [77,78]. The acoustic-wave equation in a unidirectional shear flow has been extended to the isentropic nonhomentropic case [8], including swirl [9], allowing for high-Mach-number flow and temperature gradients. It has been solved for a linear velocity profile [79] in a homoenergetic flow; in this case, in addition to the critical layer, there are also singularities at the critical flow points at which the sound speed vanishes. This is an example of sound in an isentropic nonhomentropic shear flow for which, in addition to the critical level, there may be other singularities due to the nonuniform sound speed.

A particular case of isentropic nonhomentropic flow is the homoenergetic flow, which has constant enthalpy (Appendix A). This condition relates the sound speed to the flow velocity and thus specifies the temperature profile in the mean flow. The critical points of the mean flow, in which the sound speed vanishes, are singularities of the acoustic-wave equation. Thus, the latter (Sec. II) has three regular singularities, at the critical level and at the critical flow points, plus a singularity at infinity, which is irregular in the case of a linear shear flow. A differential equation with four regular singularities is of the Lamé or Heun type if they are all regular, and (because, in the present case, one singularity is irregular) this leads to an extended Heun differential equation (Appendix B). The acoustics of a plane's unidirectional homoenergetic shear flow (Sec. II) with a linear velocity profile (Sec. III) can be matched to a uniform stream (Sec. IV) containing a line source of sound (Appendix C). The sound field emitted by the source

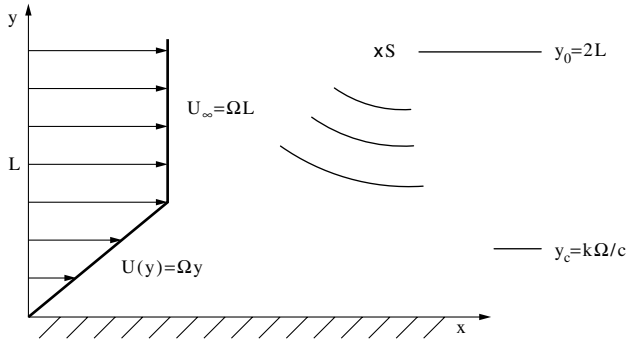

Fig. 1 Sound wave of frequency ω and horizontal wave number k propagating in a linear shear flow of vorticity Ω, matched to a uniform stream of arbitrary velocity U_∞ to represent a boundary layer of thickness $L = U_\infty/\Omega$.

outside the nonisothermal boundary layer (Fig. 1) is partially reflected and partially transmitted; the refraction effects depend on the velocity and the temperature or sound speed profiles in the boundary layer (Fig. 2). The acoustic pressure is calculated from series solutions converging in the whole flow region (Fig. 3) for 15 combinations (Table 1) of the three dimensionless parameters:

1) The first parameter is the local freestream Mach number calculated from the freestream velocity and the freestream sound speed (which is lower than the stagnation sound speed).

2) The second parameter is the ratio of horizontal phase speed to the sound speed in the freestream, which is related to the direction of propagation and the evanescence conditions.

3) The third parameter is the Strouhal number or ratio of the wave frequency to the vorticity, which is constant in the linear shear velocity profile in the boundary layer. In these 15 cases of homoenergetic (i.e., isentropic nonhomentropic) flow, the modulus and the phase of the acoustic pressure is plotted (Figs. 4–6) versus the distance from the wall (made dimensionless by dividing the boundary-layer thickness). The sound source is placed at a distance from the wall of twice the boundary-layer thickness; the same distance from the wall was also used in a comparison of homentropic and homoenergetic shear flows (Figs. 7 and 8) that show little difference at low Mach numbers as concerns sound transmission. At higher Mach numbers, the nonuniform sound speed in the nonhomentropic case is associated with temperature gradients that cause additional sound refraction, implying a significant reduction of acoustic pressure at the wall (Sec. V).

II. Acoustic Wave Equation in High-Speed Homoenergetic Shear Flow

Consider a unidirectional shear flow,

$$U = U(y)e_x \tag{1a}$$

$$\frac{\mathrm{d}}{\mathrm{dt}} \equiv \frac{\partial}{\partial t} + U \cdot \nabla = \frac{\partial}{\partial t} + U(y)\frac{\partial}{\partial x} \tag{1b}$$

for which the material derivative is given by Eq. (1b); the inviscid momentum

$$\frac{\partial U}{\partial t} + (U \cdot \nabla)U + \rho^{-1}\nabla p = 0 \tag{2a}$$

$$[p = \text{const} = p_0] \tag{2b}$$

leads to constant gas pressure Eq. (2b), regardless of whether the mass density is constant or not. For a homentropic mean flow, because the entropy is constant ($s = \text{const} \equiv s_0$), it follows that every other mean flow quantity [e.g., mass density ($\rho = \text{const} \equiv \rho_0$) and sound speed ($c = \text{const} \equiv c_0$)] is also constant; in the case of isentropic but nonhomentropic mean flow, the entropy can vary across (but not along) streamlines $s(y)$, and thus the mass density

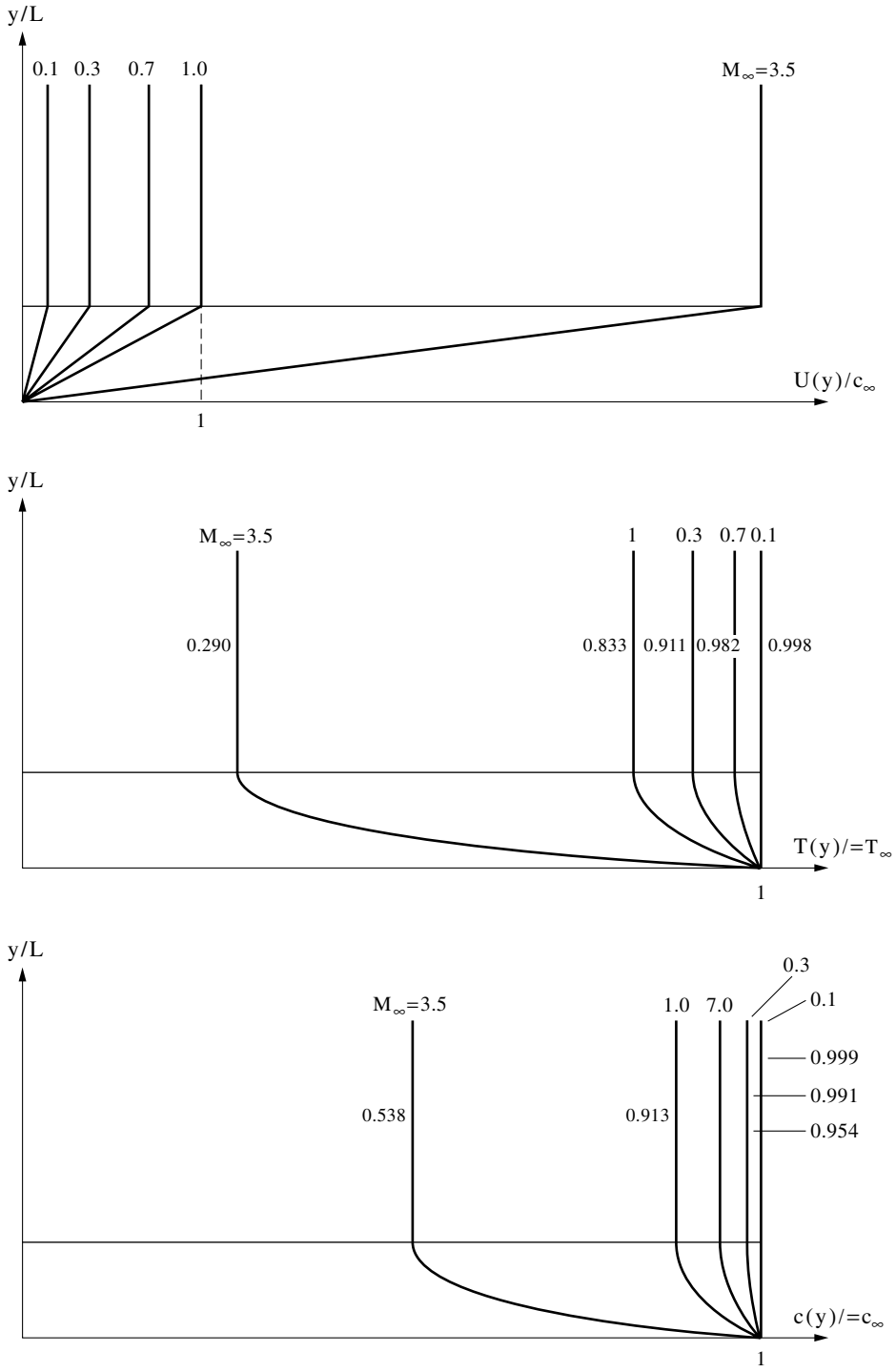

Fig. 2 Homoenergetic unidirectional shear flow with a linear velocity profile [Eq. (33)] in the boundary layer matched to a uniform stream: a) the condition of constant stagnation enthalpy specifies the corresponding b) temperature [Eq. (60)] and c) sound speed [Eq. (56b)] profiles.

$\rho(y)$ and the sound speed $c(y)$ can also vary across streamlines. In this case, it can be shown that the acoustic-wave equation satisfied by the pressure [8,76] is

$$\frac{\mathrm{d}}{\mathrm{d}t}\left(\frac{1}{c^2}\frac{\mathrm{d}^2 p}{\mathrm{d}t^2} + \nabla(\log\rho_0)\cdot\nabla p - \nabla^2 p\right) + 2U'\frac{\partial^2 p}{\partial x\,\partial y} = 0 \quad (3)$$

which is of the third order due to coupling the two acoustic modes to vorticity. Taking into account that the adiabatic sound speed is given for a perfect gas by Eq. (4a), for a constant mean flow pressure an adiabatic exponent follows [Eq. (4b)]:

$$c^2 = \gamma p/\rho \quad (4a)$$

$$p,\ \gamma = \text{const}:\ \nabla(\log c^2) = -\nabla(\log\rho) \quad (4b)$$

In particular, for a perfect gas [Eq. (5a)], the sound speed [Eq. (5b)] leads to Eq. (5c):

$$R,\ p_0 = \text{const}:\ p_0 = R\rho T \quad (5a)$$

$$c^2 = \gamma RT \quad (5b)$$

$$\nabla(\log c^2) = \nabla(\log T) \quad (5c)$$

Using Eq. (4b) in Eq. (3), it follows that the acoustic pressure perturbation in a high-speed unidirectional shear flow satisfies the wave equation,

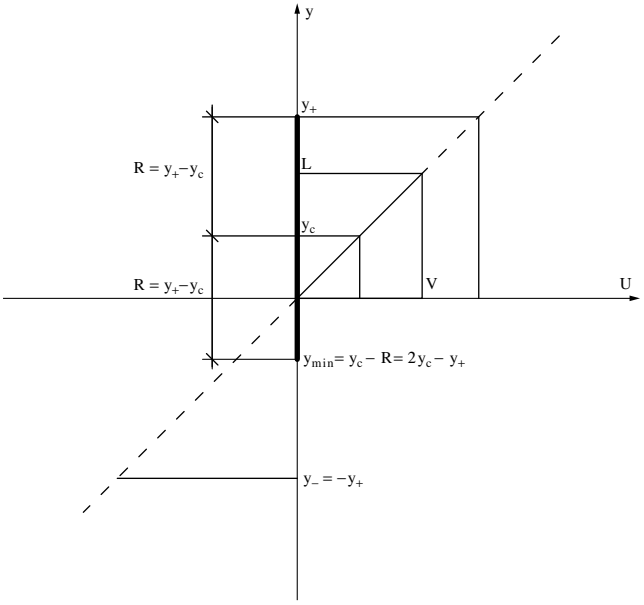

Fig. 3 Linear velocity profile in the boundary layer matched to a uniform freestream. In the case of a critical level in the boundary layer, the radius of convergence R of the series solution around the critical level is determined by the nearest singularity, which is the upper critical flow point. Thus, the region of validity of the solution is below $y_+ \equiv y_{\max}$ and above $y_{\min}$.

$$\frac{\mathrm{d}}{\mathrm{d}t}\left\{\frac{1}{c^2}\frac{\mathrm{d}^2 p}{\mathrm{d}t} - \nabla(\log c^2)\cdot\nabla p - \nabla^2 p\right\} + 2U'\frac{\partial^2 p}{\partial x\,\partial y} = 0 \quad (6)$$

in agreement with a longer derivation [5,20], which includes source terms.

Because the mean flow properties depend only on the transverse coordinate y (i.e., the mean flow is steady and longitudinally uniform), it is convenient to use a Fourier decomposition in time t and a longitudinal coordinate x,

$$p(x, y, t) = \int_{-\infty}^{+\infty}\int P(y; k, \omega)e^{i(\omega t - kx)}\,\mathrm{d}\omega\,\mathrm{d}k \quad (7)$$

where $P(y; k, \omega)$ denotes the acoustic pressure perturbation spectrum for a wave of frequency ω and for a longitudinal wave number k at position y. The dependence of the acoustic pressure on the latter is generally not sinusoidal [i.e., it is specified by substituting Eq. (7) in Eq. (6)]; namely,

$$(\omega - kU)P'' + 2[kU' + (\omega - kU)c'/c]P' + (\omega - kU)[(\omega - kU)^2/c^2 - k^2]P = 0 \quad (8)$$

where the following have been used:

$$\frac{\partial}{\partial t} \to i\omega \quad (9a)$$

$$\frac{\partial}{\partial x} \to -ik \quad (9b)$$

$$\frac{\mathrm{d}}{\mathrm{d}t} \to i(\omega - kU) \quad (9c)$$

To solve the wave equation (8), it is necessary to specify [despite the profile of the mean flow velocity $U(y)$] the profile of the sound speed $c(y)$. For a perfect gas, the choice of the sound-speed profile $c(y)$ is equivalent to the choice of a temperature profile $T(y)$; most of the exact solutions of the acoustic-wave equation in a unidirectional shear flow assume a linear velocity profile [32,70–74] and a homentropic flow (i.e., constant entropy). In this case, the sound speed is constant, and the wave equation (8) reduces to the well-known form [1–7],

$$(\omega - kU)P'' + 2kU'P' + (\omega - kU)[(\omega - kU)^2/c^2 - k^2]P = 0 \quad (10)$$

which is the one considered in all of the references previously mentioned. The derivation of Eq. (8) applies equally well to isentropic nonhomentropic mean flow, in which case the wave equation (10) holds only at a low Mach number when the sound speed is constant. In the present paper, neither the restriction to homentropic mean flow nor the restriction to low-Mach-number mean flow are made, and so the wave equation (8) does not reduce to Eq. (10) (i.e., the mean flow temperature is not assumed to be uniform). Thus, the acoustic-wave equation (8) describes the propagation of sound in a nonisothermal unidirectional shear flow, if the isentropic condition is retained, but the homentropic condition is not imposed.

A possible choice of temperature profile, which is consistent with isentropic nonhomentropic mean flow, is the condition [79] of constant stagnation enthalpy; this allows ρ, T, and c to vary from one streamline to the next as a function of y. This relates the sound speed $c(y)$ and the mean flow velocity $U(y)$ at an arbitrary streamline to the stagnation sound speed c_0 by Eq. (11a), where ε is the compressibility constant [Eq. (11b)]:

$$[c(y)]^2 = c_0^2 - \varepsilon^2[U(y)]^2 \quad (11a)$$

$$\varepsilon \equiv \sqrt{(\gamma - 1)/2} \quad (11b)$$

$$T(y)/T_0 = 1 - [\varepsilon U(y)/c_0]^2 \quad (11c)$$

The corresponding temperature profile is in Eq. (11c), where T_0 is the stagnation temperature. The ratio of specific heats, at a constant pressure and volume for a perfect gas, takes the value in Eq. (12b),

Table 1 Coverage of the boundary layer by solutions around the wall ($z = 0$) and the critical level ($z = z_c$)

Figure	Case	β_∞	M_∞	z_c	$z_\pm$	R	$z_{\min}$	$z_{\max}$	Solution around
Fig. 4	1	2.0	0.7	2.857	±3.347	2.857	−2.857	+2.857	$z = 0$
Fig. 4	2	0.5	0.7	0.714	±3.347	2.633	−1.919	3.347	$z = z_c$
Fig. 4	3	−0.1	0.7	−0.143	±3.347	3.204	−3.347	3.061	$z = z_c$
Fig. 4	4	−4.0	0.7	−5.714	±3.347	2.990	−3.347	3.347	$z = 0$
Fig. 5	5	4.0	1.0	4.000	±2.449	2.449	−2.449	2.449	$z = 0$
Fig. 5	6	1.0	1.0	1.000	±2.449	1.449	−0.449	2.449	$z = z_c$
Fig. 5	7	−0.5	1.0	−0.500	±2.449	1.949	−2.449	1.449	$z = z_c$
Fig. 6	8	3.0	3.5	0.857	±1.187	0.857	−0.857	0.857	$z = 0$
						0.330	0.527	1.187	$z = z_c$
Fig. 6	9	2.0	3.5	0.571	±1.187	0.616	−0.045	1.187	$z = z_c$
Fig. 6	10	−4.0	3.5	−1.142	±1.187	1.142	−1.142	1.142	$z = 0$
Figs. 7 and 8	11	4.0	0.1	40.000	±22.383	22.383	−22.383	22.383	$z = 0$
Figs. 7 and 8	12	4.0	0.3	13.333	±7.520	7.520	−7.520	7.526	$z = 0$
Figs. 7 and 8	13	4.0	0.7	5.714	±3.347	3.347	−3.347	3.347	$z = 0$
Figs. 7 and 8	14	4.0	1.0	4.000	±2.449	2.449	−2.449	2.449	$z = 0$
Figs. 7 and 8	15	4.0	3.5	1.143	±1.187	1.143	−1.143	1.143	$z = 0$

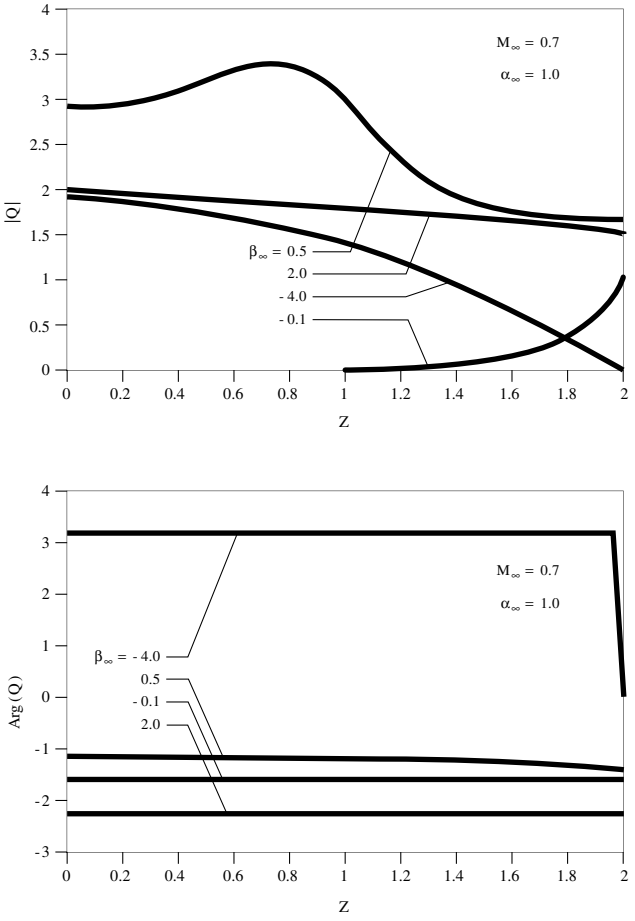

Fig. 4 Acoustic pressure versus distance from a rigid wall for a) amplitude and b) phase, made dimensionless by dividing the boundary-layer thickness for a homoenergetic flow with a linear velocity profile (matched to an uniform stream of high subsonic Mach number $M_\infty = 0.7$). Sound from a line source at a distance from the wall equal to the double of the boundary-layer thickness. Wave frequency equal to vorticity $\alpha_\infty = 1$ and four values of [Eq. (37b)] ratio of horizontal phase speed to sound speed in freestream, including positive $\beta_\infty > 0$ and negative $\beta_\infty < 0$ horizontal wave number k corresponding, respectively, to downstream and upstream propagation.

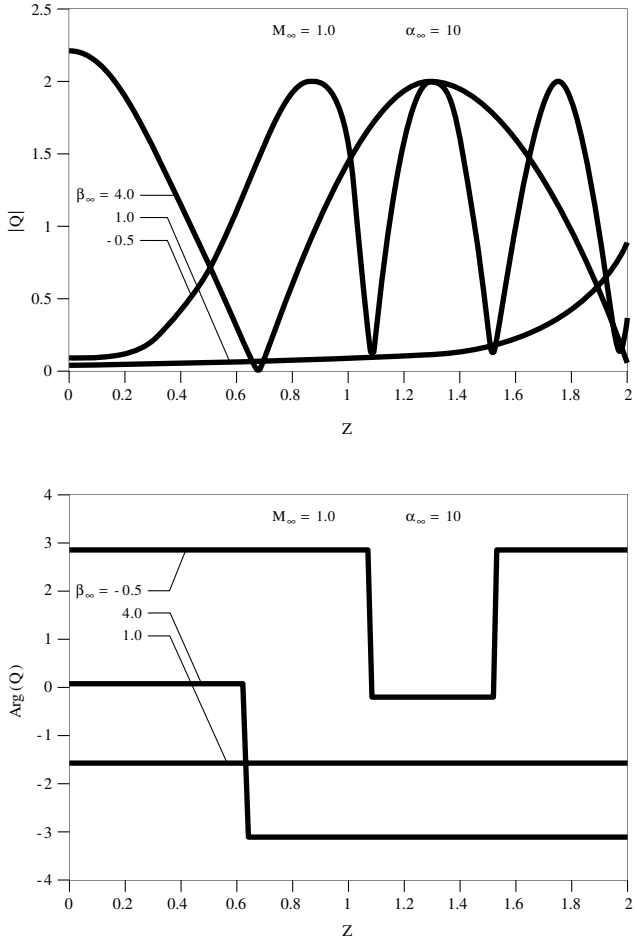

Fig. 5 As in Fig. 4, for sonic freestream $\beta_\infty = 1$, the wave frequency is much higher than the vorticity $\alpha_\infty = 10$ and the three values of β_∞ in Eq. (37b).

where N is [Eq. (12a)] the number of degrees of freedom of a molecule:

1) A monatomic gas ($N = 3$) gives $\gamma = 5/3$.

2) A diatomic gas or a polyatomic gas with molecules along a line $N = 5$ leads to $\gamma = 7/4$ (e.g., air consisting of diatomic nitrogen N_2 and oxygen O_2 in ambient conditions).

3) For a three-dimensional polyatomic molecule, $N = 6$ leads to $\gamma = 4/3$ in.

$$N = 3,\ 5,\ 6 \tag{12a}$$

$$\gamma \equiv C_p/C_v = 1 + 2/N = 5/3,\ 7/5,\ 4/3 \tag{12b}$$

The values in Eq. (12b) correspond to

$$N = 3,\ 5,\ 6 \tag{13a}$$

$$\varepsilon = \sqrt{(\gamma-1)/2} = 1/\sqrt{N} = 1/\sqrt{3},\ 1/\sqrt{5},\ 1/\sqrt{6} = 0.577,\ 0.447,\ 0.408 \tag{13b}$$

for the compressibility constant. For gas mixtures and imperfect gases, other values of γ, and hence ε, are possible.

In the case of a boundary layer (Fig. 1), as the mean flow velocity increases from zero at the wall [$U(y) = 0$] to the freestream velocity far away [$U(\infty) = U_\infty$], the sound speed c_0 and the temperature reduce from Eqs. (14a) and (14b), leading to a negative temperature gradient:

$$c_0^2 = \gamma RT \tag{14a}$$

$$c_\infty^2 = \gamma RT_\infty = c_0^2 - \varepsilon^2 U^2 \tag{14b}$$

$$\frac{\mathrm{d}T}{\mathrm{d}y} = -2\varepsilon^2 U \frac{\mathrm{d}U}{\mathrm{d}y} < 0 \tag{14c}$$

Thus, the case of homoenergetic shear flow corresponds to a negative temperature gradient. The acoustic-wave equation (8) in a high-Mach-number homoenergetic shear flow

$$(\omega - kU)(c_0^2 - \varepsilon^2 U^2)P'' + 2U'[k(c_0^2 - \varepsilon^2 U^2) - \varepsilon^2 U(\omega - kU)]P' + (\omega - kU)[(\omega - kU)^2 - k^2(c_0^2 - \varepsilon^2 U^2)]P = 0 \tag{15}$$

has four singularities:

1) The first singularity is a critical level at which the Doppler shifted frequency vanishes [Eq. (16a)],

$$0 = \omega_*(y_c) \equiv \omega - kU(y_c) \tag{16a}$$

$$U(y_c) = \omega/k \tag{16b}$$

[i.e., the mean flow velocity equals the acoustic phase speed calculated from the horizontal wave number in Eq. (7)]

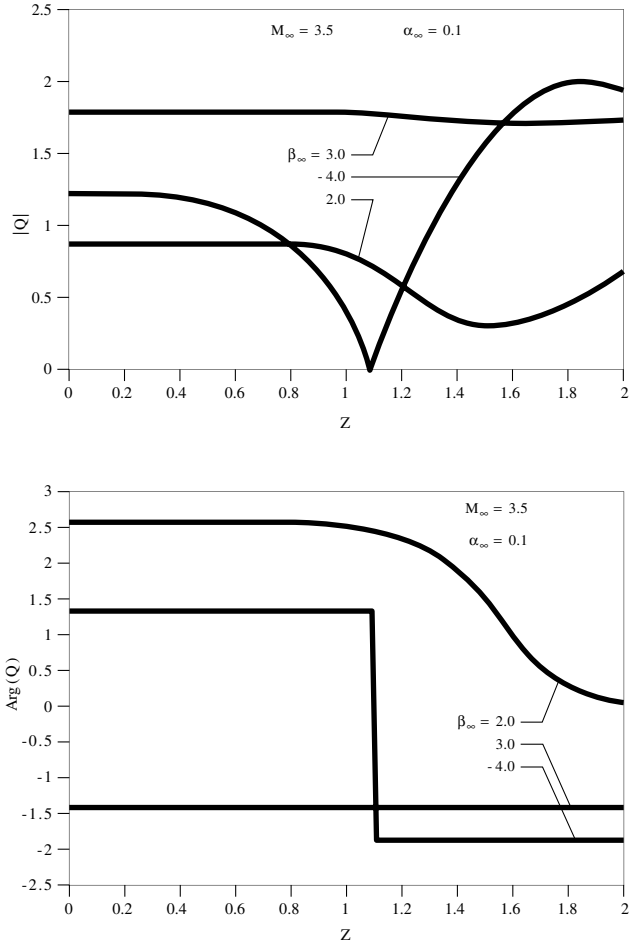

Fig. 6 As in Fig. 4, for supersonic freestream $M_\infty = 3.5$, the wave frequency is much smaller than the vorticity $\alpha_\infty = 0.1$ and the three values of β_∞ in Eq. (37b).

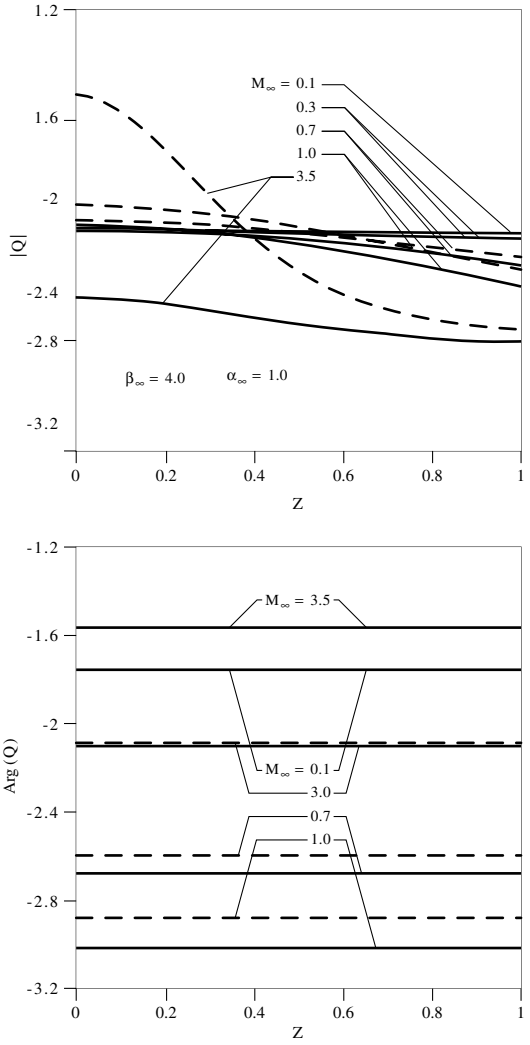

Fig. 7 Comparison (as in Fig. 4) of the sound fields due to a line source for homoenergetic (solid line) and homentropic (dotted line) shear flows and for low speed $M_\infty = 0.1$, incompressible $M_\infty = 0.3$, subsonic $M_\infty = 0.7$, sonic $M_\infty = 1$, and supersonic $M_\infty = 3.5$ freestreams. The wave frequency is equal to the vorticity $\alpha_\infty = 0.1$ and $\beta_\infty = 4$ in Eq. (37b).

2) The second and third singularities are the two critical flow points at which the sound speed vanishes [Eq. (16a)],

$$0 = c(y_\pm) \tag{16c}$$

$$U(y_\pm) = \pm c_0/\varepsilon = \pm\sqrt{2/(\gamma-1)}c_0 = \pm c_0\sqrt{N} \tag{16d}$$

corresponding to Eqs. (11–16) for a perfect gas, for which the molecules have N degrees of freedom.

3) The fourth singularity is the point at infinity $y = \pm\infty$.

III. Critical Level for Sound and Critical Flow Points

The homoenergetic mean flow is one of the simplest choices of nonhomentropic flow in which the energy equation takes a simplified form (Appendix A); it allows an assessment of nonisothermal effects on the propagation of sound in shear flows. One effect already apparent is that the sound speed in Eq. (11a) is not constant (i.e., it depends on the velocity profile of the unidirectional shear flow); hence, the sound speed is a function of the distance from the wall, leading to refraction effects and the appearance of the additional singularities [Eqs. (16c) and (16d)] in the wave equation. Most of the literature considers the propagation of sound in a shear flow in homentropic conditions, with the simplest velocity profile being the linear case [33,70–74]. This velocity profile is also taken in the present study of sound propagation in a homoenergetic [79] shear flow. Thus, to complete the specification of the wave equation (14), a linear shear flow (Fig. 1) is considered,

$$U(y) = \Omega y \tag{17a}$$

$$\Omega \equiv \frac{\mathrm{d}U}{\mathrm{d}y} = \text{const} \tag{17b}$$

for which the vorticity is constant [Eq. (17b)] and specifies the position in Eq. (16a) of the critical layer in Eq. (12b); namely,

$$y_c = \omega/(\Omega k) \tag{18a}$$

$$y_\pm = \pm c_0/\varepsilon\Omega \tag{18b}$$

The location of the critical layer [Eq. (18a)] is generally distinct from the position [Eq. (18b)] of the two critical flow points [Eq. (16d)]. Coincidence would be possible only for $y_c = y_+$ if the horizontal phase speed had a precise relation to the stagnation sound speed $\omega/k = c_0/\varepsilon$ and for propagation in the positive x direction $k > 0$ or, alternatively, $y_c = y_-$ for propagation in the negative x direction $k < 0$. The change of the independent variable

$$\xi \equiv y/y_c = kU/\omega = \Omega k y/\omega \tag{19a}$$

$$J(\xi;\, k,\, \omega) = P(y;\, k,\, \omega) \tag{19b}$$

places the critical level at a point of unity $\zeta_c = 1$ and transforms the wave equation (15) to

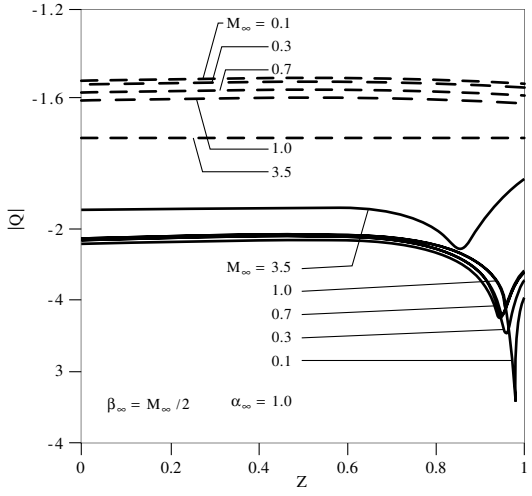

a)

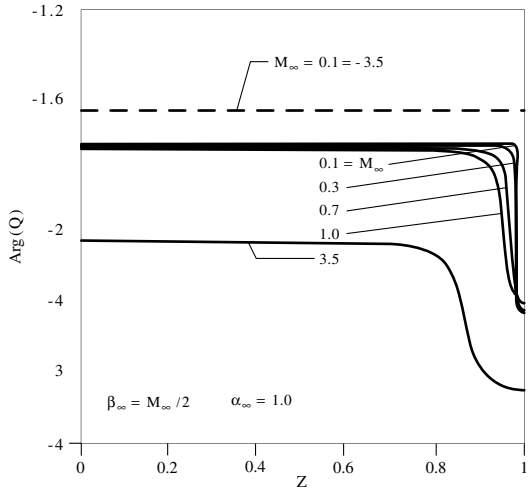

b)

Fig. 8 As in Fig. 7, with the relation $\beta_\infty = M_\infty/2$ to ensure that there is a critical level in the middle of the boundary layer $y_c = L/2$.

$$(1-\Lambda^2\xi^2)(1-\xi)J'' + 2(1-\Lambda^2\xi)J' - \alpha(1-\xi)[1-\Lambda^2\xi^2 - \beta^2(1-\xi)^2]J = 0 \tag{20}$$

involving three dimensionless parameters,

$$\alpha \equiv (\omega/\Omega)^2 \tag{21a}$$

$$\beta \equiv \omega/(c_0 k) \tag{21b}$$

$$\Lambda \equiv \varepsilon\omega/(c_0 k) \tag{21c}$$

namely,

1) The first parameter is the square of the ratio of the wave frequency ω to the mean flow vorticity Ω, which is smaller for the larger shear flow effect.

2) The second parameter is the ratio of horizontal phase speed $u = \omega/k$ to sound speed c_0 (viz., $\beta = u/c_0$), so that $\beta = 1$ for horizontal propagation, $\beta > 1$ for transversely propagating waves $\omega > kc_0$, and $\beta < 1$ for transversely evanescent waves.

3) The third parameter is $\Lambda = 0$ for low-Mach-number flows $c = c_0$, $\gamma = 1$, or $\varepsilon = 0$ in Eqs. (11a) and (11b), so that $\Lambda \neq 0$ is a measure of the high-speed effects.

The change of the independent variable

$$\zeta \equiv (\xi - 1)/(1/\Lambda - 1) \tag{22a}$$

$$R(\zeta) \equiv J(\xi;\, k,\, \omega) \tag{22b}$$

shifts the regular singularities at the critical level, and the critical flow points from Eqs. (18a) and (18b) in terms of y to Eq. (23a) in terms of ξ in Eq. (19a), and to Eq. (23b) in terms of ζ in Eq. (22a),

$$\xi_c,\, \xi_\pm = 1,\ \pm 1/\Lambda \tag{23a}$$

$$\zeta_c,\, \zeta_+,\, \zeta_- = 0,\, 1,\, (\Lambda+1)/(\Lambda-1) \equiv F \tag{23b}$$

and lead to the differential equation:

$$\zeta(\zeta-1)(\zeta-F)R'' - 2[F - \Lambda\zeta/(\Lambda-1)]R' - \alpha(1-1/\Lambda)^2\zeta[(\zeta-1)(\zeta-F) + \beta^2\zeta^2/\Lambda^2]R = 0 \tag{24}$$

The point at infinity could be expected to be an irregular singularity of the wave equation, because the mean flow velocity diverges there. It can be confirmed that the point at infinity is an irregular singularity of degree two by performing the change of variable,

$$\eta = 1/\zeta \tag{25a}$$

$$I(\eta) = R(\zeta) \tag{25b}$$

which transforms the wave equation (24) to

$$\eta(1-\eta)(1-F\eta)I'' + 2[1 - 3\Lambda\eta/(\Lambda-1) + 2F\eta^2]I' - \eta^{-3}\alpha(1-1/\Lambda)^2[(1-\eta)(1-F\eta) + \beta^2/\Lambda^2]I = 0 \tag{26}$$

The point at infinity ($y,\, \xi,\, \zeta = \infty$) is mapped to the origin $\eta = 0$ in Eq. (25a) and, if the coefficient of I'' is η^2, then I has a coefficient η^{-2}, showing that $\eta = 0$ is an irregular singularity of degree two. The differential equation (24) has three regular and one irregular singularity, and it is an extended form of Heun's or Lamé's differential equation, which has four regular singularities (Appendix B). In the neighborhood of each singularity, there is a linearly independent pair of solutions for which the radius of convergence is limited by the nearest singularity. The wave field is specified in each of these regions by a linear combination of two linearly independent solutions; the arbitrary constants are determined from two boundary conditions. Depending on the location of the singularities, several pairs of solutions may have to be matched to cover the whole flow region. For example, because both the origin $\xi = 0$ and the critical level $\xi = 1$ are regular singularities, the solutions exist as the Frobenius–Fuchs series, with the unit radius of convergence; the solution around the origin is given is Appendix B for the generalized Heun's equation, of which Eq. (24) is a particular case.

A similar method applies to Eq. (24), leading to a solution [79] around the critical level, which is a linear combination,

$$Y \equiv y/y_c - 1 = \xi - 1 = \zeta(1-\Lambda)/\Lambda \tag{27a}$$

$$R(\zeta) \equiv R[\Lambda Y/(1-\Lambda)] \equiv Q(Y) = AQ_1(Y) + BQ_2(Y) \tag{27b}$$

with arbitrary constants A and B of the functions of two kinds:

1) The first kind,

$$Q_1(Y) = \sum_{n=0}^{\infty} a_n(3)\left(\frac{\Lambda Y}{1-\Lambda}\right)^{n+3} \tag{28}$$

vanishes at the critical level.

2) The second kind,

$$Q_2(Y) = Q_1(Y)\log[\Lambda Y/(1-\Lambda)] + Q_{22}(Y) \tag{29}$$

has a logarithmic singularity at the critical level, dominated by Eq. (28), and involves a complementary function,

$$Q_{22}(Y) = \sum_{n=0}^{\infty} b_n(0)\left(\frac{\Lambda Y}{1-\Lambda}\right)^n \tag{30}$$

which is finite at the critical level. The coefficients in Eq. (28) satisfy [79] the recurrence formula:

$$\begin{aligned} &F(n+\sigma+1)(n+\sigma-2)a_{n+1}(\sigma) \\ &\quad = 2[\Lambda/(\Lambda-1)](n+\sigma)(n+\sigma-2)a_n(\sigma) + [\alpha F(1-1/\Lambda)^2 \\ &\qquad - (N+\sigma-1)(N+\sigma-2)]a_{n-1}(\sigma) \\ &\qquad - \alpha(1-1/\Lambda)^2[(1+F)a_{n-2}(\sigma) - (1+\beta^2/\Lambda^2)a_{n-3}(\sigma)] \end{aligned} \tag{31}$$

The coefficients of Eq. (30) are specified by

$$b_n(0) = a_n(0) + \frac{\lim}{\sigma \to 0}\sigma \frac{\mathrm{d}}{\mathrm{d}\sigma}[a_n(\sigma)] \tag{32}$$

These wave fields have been illustrated for a linear velocity profile [79], and so it is sufficient to proceed to the matching with a uniform stream.

IV. Sound Source Outside a Boundary Layer

The linear shear flow is assumed before Eq. (17a) can be unbounded for the homentropic case and is limited by the critical flow points in Eq. (18b) in the homoenergetic case. In either case, the linear shear flow can be matched (Fig. 1) to a uniform stream,

$$U(y) = \begin{cases} \Omega y & \text{if } y \le L, \\ \Omega y \equiv U_\infty = \Omega L & \text{if } y \ge L \end{cases} \tag{33}$$

where $L = U_\infty/\Omega$ is the boundary-layer thickness and U_∞ is the freestream velocity. The critical layer in Eq. (18a) occurs within the boundary layer if $y_c < L$ or $\omega < \Omega kL$. The acoustic field inside the boundary layer has been calculated before, and the acoustic pressure $P(y; k, \omega)$ and the velocity $\sim P'(y; k, \omega)$ are to be matched across $y = L$ to the acoustic field in the freestream, thus determining the constants of integration A and B in the general solutions. In the freestream, the mean flow velocity is constant, and the wave equation (8) simplifies to

$$P''_\infty + K^2 P_\infty = S\delta(y - y_0) \tag{34}$$

where:

1) K is the vertical wave number in the freestream,

$$K \equiv |(\omega - U_\infty k)^2/c_\infty^2 - k^2|^{1/2} \tag{35}$$

involving the freestream sound speed in Eq. (14b).

2) A line source of strength S was placed in the freestream at a distance y_0 from the wall. The forced solution (Appendix C) of Eq. (36) is the first term of

$$P_\infty(y, k, \omega) = -(iS/4K)\exp[iK|y - y_0|] + C_+ \exp(-iKy) \tag{36}$$

and the second term is an upward-propagating wave of amplitude C_+, reflected from the boundary layer (because the source lies in the freestream). The source strength is chosen to be $S = i\,4$ K, and the constant C_+ is determined so as to satisfy a rigid wall condition (more details will be given in Sec. V).

The dimensionless parameters of the solution in the boundary layer [Eqs. (21a–21c)] are reconsidered, bearing in mind the matching to the uniform stream in Eq. (33):

$$\alpha_\infty \equiv (\omega/\Omega)^2 = (\omega L/U_\infty)^2 \tag{37a}$$

$$\beta_\infty \equiv \omega/(c_\infty k) \tag{37b}$$

$$\Lambda_\infty \equiv \varepsilon\omega/(c_\infty k) = \varepsilon\beta_\infty \tag{37c}$$

Thus, the ratio of the wave frequency to the vorticity becomes the Strouhal number in Eq. (37a), and Eq. (21b) and (21c) is used to show the sound speed at infinity, which is related [Eq. (38a)] to the stagnation sound speed c_0,

$$c_0^2 = c_\infty^2 + \varepsilon^2 U_\infty^2 = c_\infty^2(1 + \varepsilon^2 M_\infty^2) \tag{38a}$$

$$M_\infty \equiv U_\infty/c_\infty \tag{38b}$$

where the Mach number of the freestream was introduced [Eq. (38b)]. The distance from the wall is now made dimensionless by dividing the boundary-layer thickness,

$$z \equiv y/L = \Omega y/U_\infty \tag{39a}$$

$$z_c \equiv y_c/L = \omega/U_\infty k = \beta_\infty/M_\infty \tag{39b}$$

so that [Eq. (39b)]:

1) The critical level lies in the boundary layer $0 < z_c < 1$ if $0 < \beta_\infty < M_\infty$, which implies propagation downstream and a high Mach number

2) The critical level lies outside the flow region and above the wall $z_c > 1$ for propagation downstream and a low Mach number $\beta_\infty > M_\infty$.

3) The critical level lies outside the flow region below the wall $z_c < 0$ for propagation upstream $\beta_\infty < 0$ at any Mach number. Although the critical level lies in the physical region of interest only in case 1, in cases 1–3, it limits the radius of the convergence of other solutions (e.g., around the wall or around the critical flow points).

The lower critical flow point z_- lies below the wall [Eq. (18b)], and the upper critical flow point

$$\begin{aligned} z_+ &\equiv y_+/L = c_0/(\varepsilon\Omega L) = [c_\infty/(U_\infty\varepsilon)]\sqrt{1+\varepsilon^2 M_\infty^2} \\ &= \sqrt{1 + 1/(M_\infty\varepsilon)^2} > 1 \end{aligned} \tag{40}$$

lies above the boundary layer. The amplitude and the phase of the acoustic pressure are plotted as a function of distance from the wall (Figs. 4–8) in the 15 cases listed in Table 1. Table 1 shows the 15 combinations of the freestream Mach number [Eq. (38b)] and the ratio [Eq. (37b)] of the horizontal phase speed to the sound speed used for the plots of acoustic pressure in Figs. 4–8. In each case, the locations of the critical level and the critical flow points are indicated. These locations determine the region of convergence of the solutions around the wall ($z = 0$) and around the critical level ($z = z_c$). In most cases, the whole boundary layer is covered by one solution [viz., (1, 4, 5, 10–15)], by the solution around the wall, and (2, 3, 6, 7, 9) by the solution around the critical level. In case 8, both solutions are needed to cover the whole boundary layer, with matching in the overlapping part of their region of validity. In all of these cases, it is sufficient to use the series solutions around the critical level (Sec. III) or around the wall (Appendix B). In cases 1, 4, 5, and 10–15, both the critical level and the critical flow points are at a distance above or below the wall, greater than the thickness of the boundary layer $|z_\pm| > 1 < |z_c|$; thus, the solution around the wall $z = 0$ covers the whole flow region $0 \le |z| \le 1$. In all of the remaining cases (2, 3, 6, 7, 9) except 8, the distance of the critical level from the wall is less than that of the critical flow points and is less than the thickness of the boundary layer. If the critical level is (Fig. 3) inside the boundary layer [Eq. (41a)]:

1) The nearest singularity is the upper critical flow point, which determines the radius of convergence [Eq. (41b)] of the solution around the critical level.

2) The solution around the critical level is valid in the range [Eq. (41c)], which includes the boundary layer above the critical level.

3) The latter also includes the boundary layer below the critical level and up to the wall if $y_{\min} < 0$, in Eq. (41c):

$$0 < z_c < z_+ > 1 \tag{41a}$$

$$R = z_+ - z_c \tag{41b}$$

$$0 > z_{\min} = 2z_c - z_+ = z_c - R < z < z_c + R = z_+ \equiv z_{\max} \tag{41c}$$

A similar reasoning applies for a critical level below the wall $-1 \leq \beta_\infty \leq 1 + M_\infty$. In case 8, neither the solution around the wall nor that around the critical level alone cover the whole flow region; together, they cover the whole boundary layer, including an overlapping region at which they can be matched.

Using Eqs. (37) and (38b) in the vertical wave number [Eq. (35)],

$$K \equiv k\sqrt{(\beta_\infty - M_\infty)^2 - 1} \tag{42a}$$

it follows that it is imaginary; that is, the waves are evanescent in the freestream if

$$M_\infty - 1 \leq \beta_\infty \leq 1 + M_\infty \tag{42b}$$

The sound field, due to a time harmonic line source (Fig. 1) outside an homoenergetic boundary layer with a linear velocity profile (Fig. 2), is plotted next as a function of the dimensionless distance from the wall [Eq. (39a)] in the case of homoenergetic shear flow (Figs. 4–6), including a comparison with [33] the homentropic case (Fig. 7). The general acoustic field in the linear shear flow [Eq. (27b)] is matched to the sound field [Eq. (36)] in the uniform stream as follows:

1) The coordinate Y in Eqs. (18a) and (27a) is related to z by Eqs. (39a), (39b), and (37b) by

$$1 + Y = y/y_c = \Omega k y/\omega = \Omega L k z/\omega = z(U_\infty k/\omega) = M_\infty z/\beta_\infty \tag{43}$$

2) The incident acoustic field [Eq. (36)], due to the source in the uniform stream with strength [Eq. (44a)], is expressed in terms of z in Eq. (39a) by Eq. (44b),

$$S = i4K \tag{44a}$$

$$Q_\infty(z) \equiv P_\infty(y, K, \omega) = \exp\{iKL|z - z_0|\} + C_+ \exp(-iKLz) \tag{44b}$$

where, by Eqs. (33), (37b), (38b), and (37a),

$$kL \equiv kU_\infty/\Omega = (U_\infty/\Omega)\omega/(c_\infty\beta_\infty) = (M_\infty/\beta_\infty)(\omega/\Omega) = M_\infty\sqrt{\alpha_\infty}/\beta_\infty \tag{45a}$$

thus, from Eq. (42a),

$$KL = (M_\infty\sqrt{\alpha_\infty}/\beta_\infty)\sqrt{(\beta_\infty - M_\infty)^2 - 1} \tag{45b}$$

3) The acoustic pressure and velocity are continuous at $y = L$ or $z = 1$, or $Y = M_\infty/\beta_\infty - 1$ in Eq. (43), so that Eqs. (27b) and (44b) are equal together with their derivatives:

$$Q_\infty(1) = AQ_1(M_\infty/\beta_\infty - 1) + BQ_2(M_\infty/\beta_\infty - 1) \tag{46a}$$

$$Q'_\infty(1) = AQ'_1(M_\infty/\beta_\infty - 1) + BQ'_2(M_\infty/\beta_\infty - 1) \tag{46b}$$

4) The preceding relations in Eqs. (46a) and (46b) specify A and B in terms of C_+, and the latter is determined by the rigid wall boundary condition $Q'(-1) = 0$.

V. Effect of Mach Number, Vorticity, and Direction of Propagation

The parameter β_∞ in Eq. (37b) is interpreted most simply in the case of a plane wave of frequency ω in a medium at rest with sound speed c_∞, for which the horizontal wave number is

$$k = (\omega/c_\infty)\cos\theta_\infty \tag{47a}$$

$$\beta_\infty = \omega/(c_\infty k) = \sec\theta_\infty \tag{47b}$$

The parameter in Eq. (47b) thus specifies the angle of the direction of propagation with the horizontal. It specifies the vertical wave number,

$$M_\infty = 0 \tag{48a}$$

$$K = (\omega/c_\infty)\sin\theta_\infty = \beta_\infty k\sqrt{1 - \beta_\infty^{-2}} = k\sqrt{\beta_\infty^2 - 1} \tag{48b}$$

in agreement with Eq. (42), in the absence of mean flow [Eq. (48a)]. Then, when a plane wave corresponds to

$$M_\infty = 0 \tag{49a}$$

$$\beta_\infty > 1 \tag{49b}$$

$$p_\infty(x, y, z) = A\exp[i(\omega t - kx - Ky)] = A\exp\left[i(\omega/c_\infty)(c_\infty t - x/\beta_\infty - y\sqrt{1 - \beta_\infty^{-2}})\right] \tag{49c}$$

there is vertical propagation for real K in Eq. (48b) or $\beta_\infty \geq 1$ in Eq. (49b). Instead, $\beta_\infty < 1$ leads to evanescent waves:

$$M_\infty = 0 \tag{50a}$$

$$\beta_\infty < 1 \tag{50b}$$

$$p_\infty(x, y, t) = A\exp[i(x/c_\infty)(t/c_\infty - x/\beta_\infty)] \times \exp[-(\omega/c_\infty)|\beta_\infty^{-2} - 1|^{1/2}y] \tag{50c}$$

In the presence of a uniform mean flow of Mach number M_∞, the vertical wave number in Eq. (48b) is replaced by Eq. (51),

$$K = \sqrt{(\omega/c_\infty)^2(1 - M_\infty\cos\theta_\infty)^2 - k^2} = k\sqrt{\beta_\infty^2(1 - M_\infty/\beta_\infty)^2 - 1} \tag{51}$$

in agreement with Eq. (42). A plane wave in the freestream is specified, instead of Eq. (49c), by

$$p_\infty(x, y, t) = \left\{\exp i(\omega/c_\infty)[c_\infty t - x/\beta_\infty - (y/\beta_\infty)\sqrt{(\beta_\infty - M_\infty)^2 - 1}]\right\} \tag{52}$$

The condition of propagation is real K in Eq. (51), corresponding to

$$(\beta_\infty - M_\infty)^2 > 1 \tag{53a}$$

$$\beta_\infty < M_\infty - 1 \tag{53b}$$

or

$$\beta_\infty > 1 + M_\infty \tag{53c}$$

If neither of the conditions in Eqs. (53b) and (53c) is met, then the evanescent waves [Eq. (42b)]

$$p_\infty(x, y, t) = A\exp[i\omega(t - x/c_\infty\beta_\infty)]\exp[(\omega/c_\infty)|1 - (1 - M_\infty/\beta_\infty)^2|^{1/2}y] \tag{54}$$

correspond to zones of silence.

Inside the boundary layer, there is a horizontal wave number k, as shown by the Fourier spectrum in Eq. (7). There is no vertical wave number, because the wave equation (15) has no sinusoidal solutions. The exact solutions in Eqs. (28–30) involve multiple internal reflections of all orders in the boundary layer. It is possible to choose the constants of integration (A and B) in the general solution [Eq. (27b)] to match an upward- or downward-propagating wave in the freestream:

$$p_\pm(y; k, \omega) = A_\pm\exp(\pm iKy) = A_\pm\exp(iKLY) = Q_\pm(Y) \tag{55}$$

with given amplitudes $A_{\pm}$. The boundary conditions would be similar to Eqs. (46a) and (46b), replacing Q_{∞} with Q_{-} for a downward-propagating wave and Q_{+} for an upward-propagating wave in the freestream. The boundary conditions in Eqs. (45a) and (45b), used for the following Figs. 3–7, correspond to Eq. (36); that is, a source outside the boundary layer plus a reflected wave, thus excluding incoming waves from infinity. The source is placed at a distance from the wall equal to the double of the boundary-layer thickness $y_0 = 2L$ or $z_0 = 2$; the scaling of the distance from the wall with the boundary-layer thickness [Eq. (39a)] is retained for all plots, for consistency of the representation of the mean flow (Figs. 1–3) and the sound fields (Figs. 4–8). The normalization of the distance from the wall, with regard to the thickness of the boundary layer, is convenient for the sound field [Eqs. (43–46)] in the region of nonuniform flow. The distance of the sound source from the wall appears only in the simpler sound field in the freestream. The velocity profile (Fig. 1) matches [Eq. (33)] a uniform stream of velocity U_{∞} to a zero velocity at the wall through [Eq. (33)] a boundary layer of thickness L with a linear velocity profile. The sound speed in the boundary layer [Eq. (11a)] is related to that at infinity [Eq. (14a)] by

$$0 \leq y \leq L \tag{56a}$$

$$[c(y)]^2 = c_{\infty}^2 + [(\gamma - 1)/2](U_{\infty}^2 - \Omega^2 y^2) \tag{56b}$$

In particular, the ratio of sound speeds and temperatures at the wall and the freestream is

$$(c_0/c_{\infty})^2 = T_0/T_{\infty} = 1 + [(\gamma - 1)/2]M_{\infty}^2 = 1 + M_{\infty}^2/N \tag{57}$$

where the freestream Mach number in Eq. (38b) and the number of degrees of freedom of a molecule [Eqs. (12a) and (12b)] were used.

For a diatomic perfect gas [Eq. (58a)], with the compressibility parameter in Eq. (58b), the freestream Mach numbers [Eq. (58c)]

$$N = 5 \tag{58a}$$

$$\varepsilon = 1/\sqrt{N} = 0.447 \tag{58b}$$

$$M_{\infty} = 0.1,\ 0.3,\ 0.7,\ 1.0,\ 3.5 \tag{58c}$$

correspond to the ratios of the sound speeds [Eq. (59a)] and the temperatures [Eq. (59b)] corresponding to the profiles in Fig. 3:

$$T_{\infty}/T_0 = 0.998,\ 0.982,\ 0.911,\ 0.833,\ 0.290 \tag{59a}$$

$$c_{\infty}/c_0 = 0.999,\ 0.991,\ 0.954,\ 0.913,\ 0.538 \tag{59b}$$

The temperature profile

$$T(y)/T_{\infty} = 1 + [(\gamma - 1)/2](M_{\infty}^2 - \Omega^2 y^2/c_{\infty}^2) \tag{60}$$

leads to a negative temperature gradient in dimensionless form:

$$\frac{1}{T_{\infty}}\frac{\mathrm{d}T}{\mathrm{d}z} = \frac{\mathrm{d}(T/T_{\infty})}{\mathrm{d}(y/L)} = \frac{(1-\gamma)\Omega^2 L y}{c_{\infty}^2} = -\frac{2\Omega^2 L y}{c_{\infty}^2 N} < 0 \tag{61a}$$

It vanishes at the wall and the freestream and has a maximum value in the modulus,

$$\left| T_{\infty}^{-1}\frac{\mathrm{d}T}{\mathrm{d}z}\right|_{\max} = \left| -T_{\infty}^{-1}\frac{\mathrm{dT}}{\mathrm{dz}}\right|_{z=L} = \frac{(\gamma-1)\Omega^2 L^2}{c_{\infty}^2} = \frac{M_{\infty}^2}{2N} \tag{61b}$$

at the edge of the boundary layer. The singularities of the acoustic problem are at the critical level [Eq. (39b)] and the critical flow points [Eq. (40)] at which the sound speed [Eq. (56b)] vanishes:

$$c(z_{\pm}) = 0\text{: } z_{\pm} = \pm\sqrt{1 + [2/(\gamma-1)]/M_{\infty}^2} = \pm\sqrt{1 + N/M_{\infty}^2} \tag{62}$$

The positions of the three singularities determine (Table 1) the solutions of the wave equation that are sufficient to cover the flow region.

VI. Conclusions

The first set of plots (Figs. 4–7) concern sound propagation in a homoenergetic shear flow. In the case (Fig. 4) of a high subsonic freestream $M_{\infty} = 0.7$, propagation in the freestream corresponds [Eqs. (53a–53c)] to $\beta_{\infty} < -0.3$ or $\beta_{\infty} > 1.7$. For a wave frequency equal to the vorticity $\alpha_{\infty} \equiv 1$, the amplitude (Fig. 4a) is almost uniform in the case of downstream propagation $\beta_{\infty} = 2.0$, and it decays rapidly away from the wall in the case of upstream propagation $\beta_{\infty} = -4.0$; in the cases of evanescence in the freestream, the amplitude increases slowly away from the wall for upstream $\beta_{\infty} = -0.1$, and it oscillates for downstream propagation $\beta_{\infty} = 0.5$. The phase (Fig. 4b) varies little in all cases; it is largest for upstream propagation $\beta_{\infty} = -4$ and lowest for upstream propagation $\beta_{\infty} = 2.0$, with smaller values in the modulus in the evanescent cases $\beta_{\infty} = -0.1$ and 0.5. For a sonic freestream $M_{\infty} = 1$, the propagation range [Eqs. (53b) and (53c)] in the freestream is $\beta_{\infty} < 0$ or $\beta_{\infty} > 2$. For a wave frequency much higher than the vorticity $\alpha_{\infty} = 10$, corresponding (Fig. 5) to the ray theory, there is small change in amplitude (Fig. 5a) or phase (Fig. 5b) for downstream evanescence $\beta_{\infty} = 1$; the amplitude oscillations are more marked for propagation downstream $\beta_{\infty} = 4$ and upstream $\beta_{\infty} = -0.5$, with phase jumps of π at the nodes. For a supersonic freestream $\beta_{\infty} = 3.5$, the propagating range [Eqs. (53b) and (53c)] is $\beta_{\infty} < 2.5$ or $\beta_{\infty} > 4.5$; for (Fig. 6) a frequency that is small when compared with the vorticity $\alpha_{\infty} = 0.1$, the amplitude (Fig. 6a) and the phase (Fig. 6b) vary little in the case of downstream evanescence $\beta_{\infty} = 3.0$. In the other case of downstream evanescence $\beta_{\infty} = 2$, there is significant amplitude variation and smooth phase changes. In the case of upstream propagation $\beta_{\infty} = -4$, the amplitude oscillation includes a node in the boundary layer, corresponding to a jump of π in the otherwise constant phase.

The last two plots (Figs. 7 and 8) concern a comparison of the sound field due to a line source over a rigid wall at a distance of two boundary-layer thicknesses for a boundary layer with a linear velocity profile in homentropic (dotted line) or homoenergetic (solid line) conditions. Note that the homentropic boundary layer is isothermal (i.e., has a constant sound speed everywhere); the homoenergetic shear flow [Eq. (11a)] has a sound speed [Eq. (56b)] and temperature [Eq. (60)] that, for a linear velocity profile [Eq. (33)], decreases away from the wall, leading to a negative temperature gradient, as shown in Fig. 2. The first plot concerns a case of wave frequency equal to the vorticity $\alpha_{\infty} = 1$ and the oblique upstream propagation $\beta_{\infty} = 4$, for which there is no critical level in the boundary layer (Fig. 7), because $\beta_{\infty} > M_{\infty}$ in Eq. (39b) implies $z_c > 1$. The amplitude (Fig. 7a) is almost identical for the homentropic S and the homoenergetic E cases at the low freestream Mach number $M_{\infty} = 0.1$, but the difference increases with the increasing Mach number $M_{\infty} = 0.2,\ 0.7,\ 1.0$, leading to very different values of the wall pressure in the supersonic case $M_{\infty} = 3.5$, when the acoustic pressure at the wall is much larger in the homentropic case. The reduction in sound speed in the freestream in the homoenergetic case implies that sound propagates against a sound speed increasing toward the wall, thus causing reflection and leading to a smaller amplitude at the wall. The phase (Fig. 7b) is larger for the homentropic case than for the homoenergetic case, with a small difference at the low Mach number $M_{\infty} = 0.1$ and a more noticeable difference with increasing the Mach number $M_{\infty} = 0.3$, 0.7, 1.0. The constant sound speed in the homentropic case leads to a larger phase shift than the sound speed, decreasing into the freestream in the homoenergetic case. The exception is the supersonic freestream $M_{\infty} = 3.5$, for which the phase is the same in the homentropic and homoenergetic cases. The reason is that $M_{\infty} = 3.5$ is the only case, in Fig. 7, of evanescence $\beta_{\infty} < M_{\infty} + 1$ for $\beta_{\infty} = 4.0$. Thus, for $M_{\infty} = 3.5$, the evanescent waves in the freestream have the same phase in the homentropic and the homoenergetic cases. The phases differ in the homentropic and

Table 2 Sound fields due to line source

	Parameters			Wave fields	
Case[a]	α_∞	β_∞	M_∞	$\|Q\|$	Arg Q
E	1.0	−4.0, −01, 0.5, 2.0	0.7	Fig. 4a	Fig. 4b
E	10	−0.5, 1.0, 4.0	1.0	Fig. 5a	Fig. 5b
E	0.1	−4.0, 2.0, 3.0	3.5	Fig. 6a	Fig. 6b
E or S	1.0	4.0	0.1, 0.3, 0.7, 1.0, 3.5	Fig. 7a	Fig. 7b
E or S	1.0	$M_\infty/2$	0.1, 0.3, 0.7, 1.0, 3.5	Fig. 8a	Fig. 8b

[a]S denotes homentropic and E denotes homoenergetic.

homoenergetic cases for propagation in the freestream $M_\infty + 1 < \beta_\infty = 4.0$, which includes all cases in Fig. 7 (except $M_\infty = 3.5$). The final plot (Fig. 8) again considers the wave frequency as equal to the vorticity $M_\infty = 1$, with the condition $\beta_\infty = M_\infty/2$, which places [Eq. (39b)] the critical layer $z_c = 0.5$ at the middle of the boundary layer. The amplitude (Fig. 8a) of the sound field is always larger in the homentropic case than in the homoenergetic case; it is almost uniform in the homentropic case and has a dip in the homoenergetic case. The homentropic case corresponding to the constant sound speed implies sound reflection due only to the velocity gradient in the shear flow; the reflection is stronger for the homoenergetic case, because it is then augmented by the gradient in sound speed (or temperature). With the increasing Mach number, the amplitude decreases monotonically in the homentropic case and tends to increase in the homoenergetic case. The phase (Fig. 8b) differs most between the homentropic and homoenergetic cases for the largest Mach number, and it is more uniform in the former case. The homentropic case of constant sound speed leads to a larger phase than the homoenergetic case for which the sound speed decays away from the wall; the effect is more noticeable for the larger freestream Mach number, because the change is sound speed (or the temperature gradient) is larger.

The near coincidence of the homentropic and homoenergetic cases at low Mach numbers results from the sound speed [Eq. (11a)] being nearly constant in that case, so that the wave equation (8) simplifies to the usual form [Eq. (10)]; as the Mach number increases, the extra terms in Eq. (8), when compared with Eq. (10), play a larger role. The plots concerning a line source outside a (Fig. 1) boundary layer with a linear shear velocity profile are indicated in Table 2, which can be compared with the complete Table 1 listing of the sound fields in the shear flow. The plots of the acoustic pressure in Figs. 4–8 involve a third dimensionless parameter, in addition to the two in Table 1; namely, the ratio of the wave frequency to the mean flow vorticity, which is constant in the boundary layer. Figures 4–6 concern the acoustics of a homoenergetic flow, and the Figs. 7 and 8 add a comparison with the acoustics of a homentropic flow. The sound field due to a source in a uniform stream, matched to a linear shear flow, was considered for the homentropic case [33] when the flow was isothermal. The consideration of the same unidirectional shear flow velocity profile in nonhomentropic conditions (e.g., for a homoenergetic profile) leads to a nonisothermal flow with a variable sound speed. The additional refraction effects are significant if the Mach number is supersonic, and lead to a noticeable reduction of acoustic pressure at the wall, for a homoenergetic profile when compared with an isothermal boundary layer. For subsonic Mach numbers, the temperature gradients are small and have a small effect. The velocity profile has a significant effect, even at low Mach numbers, in the presence of a critical level.

Acknowledgment

This work was supported by the European Union Brite/Euram research program in aeronautics under project APIAN (advanced propeller integration aerodynamics and noise).

Appendix A: Energy Equation for Isoenergetic and Homoenergetic Flows

The energy equation [80] is

$$\frac{\partial}{\partial t}\left(\frac{1}{2}\rho v^2 + \rho e\right) + \nabla\cdot\left[\rho\boldsymbol{v}\left(\frac{1}{2}v^2 + h\right)\right] = -\nabla\cdot(\chi\nabla T) + \frac{\partial}{\partial x_i}(v_j\sigma_{ij}) \tag{A1}$$

where e is the internal energy, h is the enthalpy, χ is the thermal conductivity, and σ_{ij} are the viscous stresses. Introducing the stagnation enthalpy,

$$b \equiv \frac{1}{2}v^2 + h = \frac{1}{2}v^2 + e + \frac{p}{\rho} \tag{A2}$$

the energy equation (A1) becomes

$$\frac{\partial}{\partial t}(\rho b - p) + \nabla\cdot(\rho b\boldsymbol{v}) = -\nabla\cdot(\chi\nabla T) + \frac{\partial}{\partial x_i}(v_j\sigma_{ij}) \tag{A3}$$

In the case of a nondissipative fluid, this simplifies to

$$\chi = 0 = \sigma_{ij}\colon\ -\frac{\partial p}{\partial t} + \rho\left(\frac{\partial b}{\partial t} + \boldsymbol{v}\cdot\nabla b\right) + b\left[\frac{\partial\rho}{\partial t} + \nabla\cdot(\rho\boldsymbol{v})\right] = 0 \tag{A4}$$

Using the equation of continuity, it follows that, for a nondissipative fluid,

$$\chi = 0 = \sigma_{ij}\colon\ \rho\frac{\mathrm{d}b}{\mathrm{d}t} - \frac{\partial p}{\partial t} = 0 \tag{A5}$$

If, in addition, the flow is isoenergetic,

$$\chi = 0 = \sigma_{ij}; \qquad \frac{\mathrm{db}}{\mathrm{dt}} = 0\colon\ \frac{\partial p}{\partial t} = 0 \tag{A6}$$

then the pressure is steady. Thus, the homoenergetic flow of a nondissipative fluid cannot support acoustic waves (i.e., they cannot exist in these conditions). However, acoustic waves can exist as perturbations of a homoenergetic flow. Note that simplifying the left-hand side of Eq. (A3), as in Eqs. (A5) and (A6), the energy equation can be written, in terms of the stagnation enthalpy [Eq. (A2)], for a dissipative fluid (in general),

$$\rho\frac{\mathrm{d}b}{\mathrm{d}t} - \frac{\partial p}{\partial t} = -\nabla\cdot(\chi\nabla T) + \frac{\partial}{\partial x_i}(v_j\sigma_{ij}) \tag{A7}$$

and for an isoenergetic flow:

$$\frac{\mathrm{d}b}{\mathrm{d}t} = 0\colon\ -\frac{\partial p}{\partial t} = -\nabla\cdot(\chi\nabla T) + \frac{\partial}{\partial x_i}(v_j\sigma_{ij}) \tag{A8}$$

The homoenergetic flow $b = \text{const}$ is a particular case of an isoenergetic flow $\mathrm{d}b/\mathrm{d}t = 0$.

Appendix B: Transformation to a Generalized Heun's Equation

The wave equation (24) is a second-order ordinary differential equation of the extended Heun type,

$$\zeta(\zeta-1)(\zeta-F)R'' + \{(A+B+1)\zeta^2 - [A+B+1 + F(C+D) - D]\zeta + FC\}R' - (E + AB\zeta + G\zeta^2 + H\zeta^3)R = 0 \tag{B1}$$

of which the original Heun type [81,82] is the particular case $G = 0 = H$. Any linear second-order differential equation with four regular singularities can be reduced to the original Heun type by placing the singularities at $\zeta = 0, 1, F$, and ∞. In the extended Heun

differential equation (B1) there are three regular singularities $\zeta = 0$, 1, and F, but the point at infinity ($\zeta = \infty$) is an irregular singularity of degree two, because $H \neq 0$; comparing Eq. (B1) with Eq. (24), it follows that four of the parameters in the extended Heun equation (B1) are given in the present problem by

$$C = 2 \tag{B2a}$$

$$E = 0 \tag{B2b}$$

$$\{G,\ H\} = (1 - 1/\Lambda)^2\alpha\{1 + F,\ -1 - \beta^2/\Lambda^2\} \tag{B2c}$$

The remaining three constants A, B, and D satisfy

$$A + B = -1 \tag{B3a}$$

$$AB = -\alpha(1 - 1/\Lambda)^2 F = \alpha(1/\Lambda^2 - 1) \tag{B3b}$$

$$D = -1 - 2\Lambda \tag{B3c}$$

where Eq. (23b) was used. Thus, A and B are the roots of

$$0 = (\vartheta - A)(\vartheta - B) = \vartheta^2 - (A + B)\vartheta + AB = \vartheta^2 + \vartheta + \alpha(1/\Lambda^2 - 1) \tag{B4}$$

That is, they are given by

$$A, B = -(1/2)\left\{1 \pm \sqrt{1 + 4\alpha(1 - 1/\Lambda^2)}\right\} \tag{B5a}$$

Note that, because Eq. (B1) is a generalization of Heun's differential equation, the properties of the latter do not generally apply to the former as a consequence of one of the singularities at infinity being irregular. Even the solutions in the Frobenius–Fuchs series in the neighborhood of regular singularities have different recurrence formulas for the coefficients, as is shown next in the case of the regular singularity at the origin. The point $\zeta = 0$ is a regular singularity of [Eq. (B1)] the original $H = 0 = G$ and extended $(G, H) \neq (0, 0)$ Heun equation, and so in its neighborhood Frobenius–Fuchs series, expansions exist:

$$|\zeta| < 1\text{: } R_\sigma(\zeta) = \sum_{n=0}^{\infty} e_n(\sigma)\zeta^{n+\sigma} \tag{B6}$$

with a radius of convergence specified by the nearest singularity $\xi = 1$. Substitution of Eq. (B5) into Eq. (B1) leads to the recurrence formula for the coefficients:

$$\begin{aligned} F(n + \sigma + 1)(n + \sigma + C)e_{n+1}(\sigma) = {} & \{(n + \sigma)[(n + \sigma)(1 + F) \\ & + A + B - D + F(C + D - 1)] + E\}e_n(\sigma) \\ & - [(n + \sigma - 1)(n + \sigma + A + B - 1) - AB]e_{n-1}(\sigma) \\ & + Ge_{n-2}(\sigma) + He_{n-3}(\sigma) \end{aligned} \tag{B7}$$

The indicial equation,

$$n = -1\text{: } F\sigma(\sigma + C - 1)e_0(\sigma) = 0 \tag{B8}$$

is the same for the original and extended Heun's equations, and it is also the same as for the Gaussian hypergeometric equation:

$$\begin{aligned} F = E = 0 = G = H; D = C\text{: } & \zeta(1 - \zeta)R'' \\ & + [C - (A + B + 1)\zeta]R' - ABR = 0 \end{aligned} \tag{B9}$$

The next two recurrence formulas [Eq. (B7)] for $n = 0$, 1 are also similar for the original and extended Heun's equations, but they are different from the Gaussian hypergeometric case. For $n \geq 2$, the recurrence formula is different in all three cases. As a final remark, note that the asymptotic expansions for the original and extended Heun's equations cannot be the same, because the point at infinity of the original (extended) Heun's equation is a regular (irregular) singularity and, thus, the solution cannot (must) have an essential singularity.

Appendix C: Time Harmonic Line Source in a Uniform Stream

The emission of sound by a time harmonic $e^{i\omega t}$ line source at position $y = y_0$ is specified by the wave equation (34), forced by the delta function and involving the wave number in Eq. (35). Using a Fourier representation for the spatial dependence of the acoustic pressure,

$$P_\infty(y;\ \bar{K},\ \omega) = \int_{-\infty}^{+\infty} \tilde{P}(\bar{K})e^{-i\bar{K}y}\ \mathrm{d}\bar{K} \tag{C1}$$

and recalling the property of the delta function,

$$2\pi\delta(y - y_0) = \int_{-\infty}^{+\infty} \exp[-i\bar{K}(y - y_0)]\ \mathrm{d}\bar{K} \tag{C2}$$

replaces the differential equation (34) by an algebraic relation:

$$[K^2 - \bar{K}^2]\tilde{P}(\bar{K}) = (S/2\pi)\exp(i\bar{K}y_0) \tag{C3}$$

Substituting Eq. (C3) into Eq. (C1),

$$P_\infty(y;\ k;\ \omega) = \frac{S}{2\pi}\int_{-\infty}^{+\infty} \frac{\exp[i\bar{K}(y_0 - y)]}{K^2 - \bar{K}^2}\ \mathrm{d}\bar{K} \tag{C4}$$

The integrand has two simple poles $\bar{K} = \pm K$ on the path of integration, corresponding (respectively) to upward-propagating $\bar{K} = -K$ and downward-propagating $\bar{K} = +K$ waves. Below the source $y < y_0$, the waves are propagating downward, so that the pole $\bar{K} = K$ is included, and the pole $\bar{K} = -K$ is excluded by suitably indenting the path of integration (Fig. C1) along the real axis; closing it by a large half-circle in the upper-half complex-$\bar{K}$ plane, the integral may be evaluated as the residue of the integrand at $\bar{K} = K$ times $i\pi$ (because the pole lies on the path of integration):

$$y_0 > y\text{: } P_\infty(y) = \frac{S}{2\pi}\pi i \lim_{\bar{K}\to K}(\bar{K} - K)\frac{e^{i\bar{K}(y_0 - y)}}{K^2 - \bar{K}^2} = -\frac{iS}{4K^2}e^{iK(y_0 - y)} \tag{C5a}$$

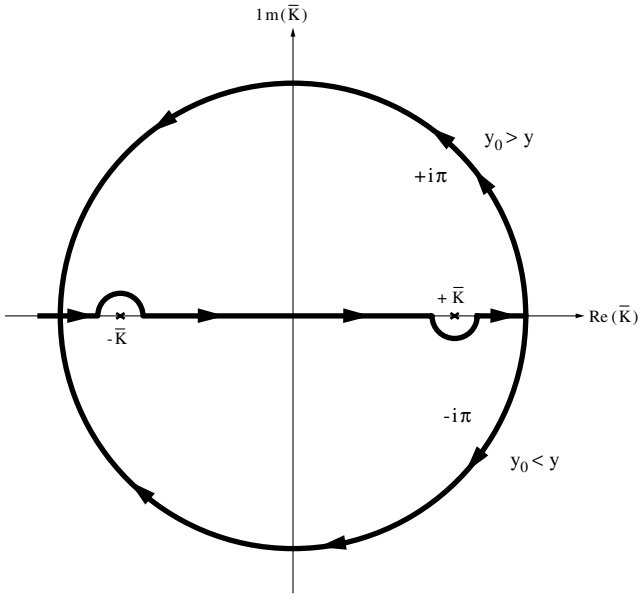

Fig. C1 Paths of integration for the evaluation of the integral [Eq. (C4)] by the residues.

Above the source $y > y_0$, the path of integration is closed by a large half-circle in the lower-half complex-$\bar{K}$ plane, so that (Fig. C1) the pole at $\bar{K} = -K$ is included, and $\bar{K} = K$ is excluded, corresponding to an upward-propagating wave and evaluation of the integral as $-i\pi$ times the residue:

$$y > y_0\text{: } P_\infty(y) = \frac{S}{2\pi}(-\pi i)\lim_{\bar{K}\to -K}(\bar{K}+K)\frac{e^{i\bar{K}(y-y_0)}}{K^2-\bar{K}^2}$$
$$= -\frac{iS}{4K}e^{iK(y-y_0)} \tag{C5b}$$

Both cases [Eqs. (C5a) and (C5b)] are included in

$$\bar{\bar{P}}_\infty(y) = -(iS/4K)\exp\{iK|y-y_0|\} \tag{C6}$$

which specifies the forced solution of Eq. (34). The free solution of the wave equation (34) is a superposition of upward- and downward-propagating waves,

$$\bar{P}_\infty(y) = C_-\exp(iKy) + C_+\exp(-iKy) \tag{C7}$$

with amplitudes, respectively, of C_+ and C_-. The sum of Eqs. (C6) and (C7) specifies the complete solution:

$$P_\infty(y) = \bar{\bar{P}}_\infty(y) + \bar{P}_\infty(y) = C_-\exp(-iKy) + C_+\exp(-iKy)$$
$$-(iS/4K)\exp\{-iK|y-y_0|\} \tag{C8}$$

To satisfy the radiation condition, $C_- = 0$ in Eq. (C8), leading to Eq. (36).

References

[1] Haurwitz, B., "Zur Theorie der Wellenbewegungen in Luft and Wasser," Vol. 6, Univ. of Leipzig, Veroff Geophysical Inst., Leipzig, Free State of Saxony, Germany, 1931, pp. 324–364.

[2] Kucheman, D., "Storüngsbewegungen in einer Gasströmung mit Grenzschicht," *Journal of Applied Mathematics and Mechanics*, Vol. 18, No. 4, 1938, pp. 207–222.

[3] Pridmore-Brown, D. C., "Sound Propagation in a Fluid Flowing Through an Attenuating Duct," *Journal of Fluid Mechanics*, Vol. 4, No. 4, 1958, pp. 393–406. doi:10.1017/S0022112058000537

[4] Mohring, W., Muller, E. A., and Obermeier, F., "Problems in Flow Acoustics," *Reviews of Modern Physics*, Vol. 55, No. 3, 1983, pp. 707–724. doi:10.1103/RevModPhys.55.707

[5] Lilley, G. M., "On Noise from Jets," AGARD CP-131, 1973, pp. 13.1–13.12.

[6] Goldstein, M. E., *Aeroacoustics*, McGraw–Hill, New York, 1976.

[7] Nayfeh, A. H., Kaiser, J. E., and Telionis, D. P., "Acoustics of Aircraft Engine-Duct Systems," *AIAA Journal*, Vol. 13, No. 2, 1975, pp. 130–153. doi:10.2514/3.49654

[8] Campos, L. M. B. C., "On 36 Forms of the Acoustic Wave Equation and in Potential Flows and Inhomogeneus Media," *Applied Mechanics Reviews*, Vol. 60, 2007, No. 4, 2007, pp. 149–171. doi:10.1115/1.2750670

[9] Campos, L. M. B. C., "On 24 Forms of the Acoustic Wave Equation and in Vortical Flows and Dissipative Media," *Applied Mechanics Reviews*, Vol. 60, No. 6, 2007, pp. 291–315. doi:10.1115/1.2804329

[10] Tack, D. H., and Lambert, R. F., "Influence of Shear Flow on Sound Attenuation in Lined Ducts," *Journal of the Acoustical Society of America*, Vol. 38, No. 4, 1965, pp. 655–666. doi:10.1121/1.1909770

[11] Mariano, S., "Effect of Wall Shear Layers on the Sound Attenuation in Acoustically Lined Rectangular Ducts," *Journal of Sound and Vibration*, Vol. 19, No. 3, 1971, pp. 261–275. doi:10.1016/0022-460X(71)90688-2

[12] Hersh, A. S., and Catton, I., "Effects of Shear Flow on Sound Propagation in Rectangular Ducts," *Journal of the Acoustical Society of America*, Vol. 50, No. 3b, 1971, pp. 992–1003. doi:10.1121/1.1912725

[13] Shankar, P. N., "Acoustic Refraction by Duct Shear Layers," *Journal of Fluid Mechanics*, Vol. 47, No. 1, 1971, pp. 81–91. doi:10.1017/S0022112071000946

[14] Shankar, P. N., "Acoustic Refraction and Attenuation in Cylindrical and Annular Ducts," *Journal of Sound and Vibration*, Vol. 22, No. 2, 1972, pp. 233–246. doi:10.1016/0022-460X(72)90538-X

[15] Shankar, P. N., "Sound Propagation in Shear Layers," *Journal of Sound and Vibration*, Vol. 15, No. 2, 1972, pp. 221–232. doi:10.1016/0022-460x(72) 90537-8

[16] Eversman, W., "Effect of Boundary Layer on the Transmission and Attenuation of Sound in an Acoustically Treated Circular Duct," *Journal of the Acoustical Society of America*, Vol. 49, No. 5a, 1971, pp. 1372–1380. doi:10.1121/1.1912512

[17] Eversman, W., and Beckenmeyer, R. J., "Transmission of Sound in Ducts with Thin Shear Layers: Convergence to the Uniform Flow Case," *Journal of the Acoustical Society of America*, Vol. 52, No. 1b, 1972, pp. 216–225. doi:10.1121/1.1913082

[18] Ko, S. H., "Sound Attenuation in Acoustically Lined Circular Ducts in the Presence of Uniform Flow and Shear Flow," *Journal of Sound and Vibration*, Vol. 22, No. 2, 1972, pp. 193–210. doi:10.1016/0022-460X(72)90535-4

[19] Swinbanks, M. A., "The Sound Field Generated by a Source Distribution in a Long Duct Carrying Sheared Flow," *Journal of Sound and Vibration*, Vol. 40, No. 1, 1975, pp. 51–76. doi:10.1016/S0022-460X(75)80230-6

[20] Mani, R., "Sound Propagation in Parallel Sheared Flows in Ducts: The Mode Estimation Problem," *Proceedings of the Royal Society of London, Series A: Mathematical and Physical Sciences*, Vol. 371, No. 1746, 1980, pp. 393–412. doi:10.1098/rspa.1980.0087

[21] Ishii, S., and Kakutani, T., "Acoustic Waves in Parallel Shear Flows in a Duct," *Journal of Sound and Vibration*, Vol. 113, No. 1, 1987, pp. 127–139. doi:10.1016/S0022-460X(87)81346-9

[22] Almgren, M., "Acoustic Boundary Layer Influence in Scale Model Simulation of Sound Propagation: Theory and Numerical Examples," *Journal of Sound and Vibration*, Vol. 105, No. 2, 1986, pp. 321–327. doi:10.1016/0022-460X(86)90160-4

[23] Goldstein, M. E., "Scattering and Distortion of the Unsteady Motion on Transversely Sheared Mean Flows," *Journal of Fluid Mechanics*, Vol. 91, No. 4, 1979, pp. 601–632. doi:10.1017/S0022112079000379

[24] Goldstein, M. E., "High-Frequency Sound Emission from Moving Point Multipole Sources Embedded in Arbitrary Transversely Sheared Mean Flows," *Journal of Sound and Vibration*, Vol. 80, 1982, pp. 449–522.doi:10.1016/0022-460X(82)90495-3

[25] Myers, M. K., and Chuang, S. L., "Uniform Asymptotic Approximations for Duct Acoustic Modes in a Thin Boundary-Layer Flow," *AIAA Journal*, Vol. 22, No. 9, 1984, pp. 1234–1241. doi:10.2514/3.48562

[26] Hanson, D. B., "Shielding of Propfan Cabin Noise by the Fuselage Boundary Layer," *Journal of Sound and Vibration*, Vol. 92, No. 4, 1984, pp. 591–598. doi:10.1016/0022-460X(84)90201-3

[27] Miles, J. W., "On the Disturbed Motion of a Vortex Sheet," *Journal of Fluid Mechanics*, Vol. 4, No. 5, 1958, pp. 538–554. doi:10.1017/S0022112058000653

[28] Graham, E. W., and Graham, B. B., "Effect of a Shear Layer on Plane Waves in a Fluid," *Journal of the Acoustical Society of America*, Vol. 46, No. 1b, 1969, pp. 169–175. doi:10.1121/1.1911666

[29] Balsa, T. F., "The Far-Field of High-Frequency Convected, Singularities in Sheared Flows, with Application to Jet Noise Prediction," *Journal of Fluid Mechanics*, Vol. 74, No. 2, 1976, pp. 193–208. doi:10.1017/S0022112076001766

[30] Balsa, T. F., "Refraction and Shielding of Sound from a Source in a Jet," *Journal of Fluid Mechanics*, Vol. 76, No. 3, 1976, pp. 443–456. doi:10.1017/S0022112076000736

[31] Munt, R. M., Interaction of Sound with a Subsonic Jet Issuing from a Semi-Infinite Jet-Pipe," *Journal of Fluid Mechanics*, Vol. 83, No. 4, 1977, pp. 609–620. doi:10.1017/S0022112077001384

[32] Koutsoyannis, S. P., Karamchti, K., and Galant, D. C., "Acoustic Resonances and Sound Scattering by a Shear Layer," *AIAA Journal*, Vol. 18, No. 12, 1980, pp. 1446–1450. doi:10.2514/3.7736

[33] Jones, D. S., "The Scattering of Sound by a Simple Shear Layer," *Philosophical Transactions of the Royal Society of London,*

Series A: Mathematical and Physical Sciences, Vol. 284, No. 1323, 1977, pp. 287–328.
doi:10.1098/rsta.1977.0011

[34] Howe, M. S., "The Attenuation of Sound by a Randomly Irregular Impedance Layer," *Proceedings of the Royal Society of London, Series A: Mathematical and Physical Sciences*, Vol. 347, No. 1651, 1976, pp. 513–535.
doi:10.1098/rspa.1976.0014

[35] Campos, L. M. B. C., "On the Spectral Broadening of Sound by Turbulent Shear Layers Part 1: Scattering by Moving Interfaces and Refraction in Turbulence," *Journal of Fluid Mechanics*, Vol. 89, No. 4, 1978, pp. 723–749.
doi:10.1017/S0022112078002827

[36] Campos, L. M. B. C., "On the Spectral Broadening of Sound by Turbulent Shear Layers. Part 2: Spectral Broadening of Experimental and Aircraft Noise," *Journal of Fluid Mechanics*, Vol. 89, No. 4, 1978, pp. 751–779.
doi:10.1017/S0022112078002839

[37] Campos, L. M. B. C., "Sur la Propagation du Sons Dans les Ecoulements Non-Uniformes et Non-Stationaires," *Revue d'Acoustique*, Vol. 67, 1983, pp. 217–233.

[38] Campos, L. M. B. C., "On Waves in Gases, Part 1: Acoustics of Jets, Turbulence and Ducts," *Reviews of Modern Physics*, Vol. 58, No. 1, 1986, pp. 117–182.
doi:10.1103/RevModPhys.58.117

[39] Lighthill, M. J., "On the Energy Scattered from Interaction of Turbulence with Sound and Shock Waves," *Proceedings of the Cambridge Philosophical Society (Mathematical and Physical Sciences)*, Vol. 49, No. 3, 1953, pp. 531–548.
doi:10.1017/S0305004100028693

[40] Schmidt, D. W., and Tilmann, P. M., "Experimental Study of Sound Phase Fluctuations Caused by Turbulent Wakes," *Journal of the Acoustical Society of America*, Vol. 47, No. 5b, 1970, pp. 1310–1324.
doi:10.1121/1.1912037

[41] Ho, C. M., and Kovasznay, L. S. G., "Propagation of a Coherent Acoustic Wave Through a Turbulent Shear Flow," *Journal of the Acoustical Society of America*, Vol. 60, No. 1, 1976, pp. 40–45.
doi:10.1121/1.381047

[42] Ho, C. M., and Kovasznay, L. S. G., "Acoustical Shadowgraph," *Physics of Fluids*, Vol. 19, No. 8, 1976, pp. 1118–1123.
doi:10.1063/1.861617

[43] Campos, L. M. B. C., "Effects on Acoustic Fatigue Loads of Multiple Reflections Between a Plate and a Turbulent Wake," *Acustica*, Vol. 76, 1992, pp. 109–117.

[44] Campos, L. M. B. C., "On Viscous and Resistive Dissipation of Hydrodynamic and Hydromagnetic Waves in Atmospheres," *Journal de Mecanique Theorique et Appliquee*, Vol. 2, No. 6, 1983, pp. 861–891.

[45] Campos, L. M. B. C., "On the Spectra of Aerodynamic Noise and Aeroacoustic Fatigue," *Progress in Aerospace Sciences*, Vol. 33, Nos. 5–6, 1997, pp. 353–389.
doi:10.1016/S0376-0421(96)00009-7

[46] Campos, L. M. B. C., and Serrão, P. G. T. A., "On the Directivity and Spectra of Noise from Unheated and Heated Jets," *International Journal of Aeroacoustics*, Vol. 6, No. 2, 2007, pp. 93–126.
doi:10.1260/147547207781041886

[47] Booker, J. R., and Bretherton, F. P. A, "Critical Layer for Internal Gravity Waves in a Shear Flow," *Journal of Fluid Mechanics*, Vol. 27, No. 3, 1967, pp. 513–529.
doi:10.1017/S0022112067000515

[48] Turner, J. S., *Buoyancy Effects in Fluids*, Cambridge Univ. Press, New York, 1973.

[49] Lighthill, M. J., *Waves in Fluids*, Cambridge Univ. Press, New York, 1978.

[50] Greenspan, H. P., *Theory of Rotating Fluids*, Cambridge Univ. Press, New York, 1968.

[51] Campos, L. M. B. C., "On Three-Dimensional Acoustic-Gravity Waves in Model Non-Isothermal Atmospheres," *Wave Motion*, Vol. 5, No. 1, 1983, pp. 1–14.
doi:10.1016/0165-2125(83)90002-1

[52] Yanowitch, M., "Effect of Viscosity on Vertical Oscillations of an Isothermal Atmosphere," *Canadian Journal of Physics*, Vol. 45, 1967, pp. 2003–2008.

[53] Lyons, P., and Yanowitch, M., "Vertical Oscillations in a Viscous and Thermally Conducting Isothermal Atmosphere," *Journal of Fluid Mechanics*, Vol. 66, No. 2, 1974, pp. 273–288.
doi:10.1017/S0022112074000206

[54] Campos, L. M. B. C., "On Waves in Non-Isothermal, Compressible, Ionized and Viscous Atmospheres," *Solar Physics*, Vol. 82, Nos 1–2, 1983, pp. 355-368.
doi:10.1007/BF00145574

[55] Lin, C. C., *Hydrodynamic Stability*, Cambridge Univ. Press, New York, 1955.

[56] Drazin, P. G., and Reid, W. H., *Hydrodynamic Stability*, Cambridge Univ. Press, New York, 1981.

[57] McKenzie, J. F., "On the Existence of Critical Levels, with Application to Hydromagnetic Waves," *Journal of Fluid Mechanics*, Vol. 58, No. 4, 1973, pp. 709–723.
doi:10.1017/S0022112073002442

[58] McKenzie, J. F., "Critical Level Behaviour of Ion–Cyclotron Waves," *Journal of Plasma Physics*, Vol. 22, No. 2, 1979, pp. 361–376.
doi:10.1017/S0022377800010163

[59] Adam, J. A., "On the Occurrence of Critical Levels in Solar Magneto-Hydrodynamics," *Solar Physics*, Vol. 52, No. 2, 1977, pp. 293–307.
doi:10.1007/BF00149646

[60] Campos, L. M. B. C., "On Vertical Hydromagnetic Waves in a Compressible Atmosphere Under an Oblique Magnetic Field," *Geophysical and Astrophysical Fluid Dynamics*, Vol. 32, No. 3, 1985, pp. 217–272.
doi:10.1080/03091928508208786

[61] Campos, L. M. B. C., "On Waves in Gases, Part 2: Interaction of Sound with Magnetic and Internal Modes," *Reviews of Modern Physics*, Vol. 59, No. 2, 1987, pp. 363–462.
doi:10.1103/RevModPhys.59.363

[62] Campos, L. M. B. C., "On the Properties of Hydromagnetic Waves in the Vicinity of Critical Levels and Transition Layers," *Geophysical and Astrophysical Fluid Dynamics*, Vol. 40, No. 1, 1988, pp. 93–132.
doi:10.1080/03091928808208821

[63] Campos, L. M. B. C., and Isaeva, N. L., "On Vertical, Spinning Alfvén Waves in a Magnetic Flux Tube," *Journal of Plasma Physics*, Vol. 48, No. 3, 1992, pp. 415–434.
doi:10.1017/S0022377800016664

[64] Campos, L. M. B. C. "On Oblique Alfvén Waves in a Viscous and Resistive Atmosphere," *Journal of Physics A: General Physics*, Vol. 21, No. 13, 1988, pp. 2911–2930.
doi:10.1088/0305-4470/21/13/015

[65] Campos, L. M. B. C., "On the Dissipation of Alfvèn Waves in Uniform and Non-Uniform Magnetic Fields," *Geophysical and Astrophysical Fluid Dynamics*, Vol. 48, No. 4, 1989, pp. 193–215.
doi:10.1080/03091928908218529

[66] Campos, L. M. B. C., "Exact and Approximate Methods for Hydromagnetic Waves in Dissipative Atmospheres," *Wave Motion*, Vol. 17, No. 2, 1993, pp. 101–112.
doi:10.1016/0165-2125(93)90019-C

[67] Campos, L. M. B. C., "Comparison of Exact Solutions and the Phase Mixing Approximation for Dissipative Alfvèn Waves," *European Journal of Mechanics, B/Fluids*, Vol. 12, No. 2, 1993, pp. 187–216.

[68] Campos, L. M. B. C., "On Hydromagnetic Waves in Atmospheres with Application to the Sun," *Theoretical and Computational Fluid Dynamics*, Vol. 10, Nos. 1–4, 1998, pp. 37–70.
doi:10.1007/s001620050050

[69] Mani, R. "The Influence of Jet Flow on Jet Noise, Part 1: the Noise of Unheated Jets," *Journal of Fluid Mechanics*, Vol. 73, No. 4, 1976, pp. 773–778.
doi:10.1017/S0022112076001602

[70] Goldstein, M., and Rice, E., "Effect of Shear on Duct Wall Impedance," *Journal of Sound and Vibration*, Vol. 30, No. 1, 1973, pp. 79–84.
doi:10.1016/S0022-460X(73)80051-3

[71] Jones, D. S., "Acoustic of a Splitter Plate," *Journal of the Institute of Mathematics and Its Applications*, Vol. 21, No. 2, 1978, pp. 197–209.
doi:10.1093/imamat/21.2.197

[72] Scott, J. N., "Propagation of Sound Waves Through a Linear Shear Layer," *AIAA Journal*, Vol. 17, No. 3, 1979, pp. 237–245.
doi:10.2514/3.61107

[73] Koutsoyannis, S. P., "Characterization of Acoustic Disturbances in Linearly Sheared Flows," *Journal of Sound and Vibration*, Vol. 68, No. 2, 1980, pp. 187–202.
doi:10.1016/0022-460X(80)90464-2

[74] Campos, L. M. B. C., Oliveira, J. M. G. S., and Kobayashi, M. H., "On Sound Propagation in a Linear Shear Flow," *Journal of Sound and Vibration*, Vol. 219, No. 5, 1999, pp. 739–770.
doi:10.1006/jsvi.1998.1880

[75] Campos, L. M. B. C., and Serrão, P. G. T. A., "On the Acoustics of an Exponential Boundary Layer," *Philosophical Transactions of the Royal Society of London, Series A: Mathematical and Physical Sciences*, Vol. 356, No. 1746, 1998, pp. 2335–2379.
doi:10.1098/rsta.1998.0277

[76] Campos, L. M. B. C., and Kobayashi, M. H., "On the Reflection and Transmission of Sound in a Thick Shear Layer," *Journal of Fluid Mechanics*, Vol. 424, 2000, pp. 303–326. doi:10.1017/S0022112000002068

[77] Campos, L. M. B. C., "On the Singularities and Solutions of the Extended Hypergeometric Equation," *Integral Transforms and Special Functions*, Vol. 9, No. 2, 2000, pp. 99–120. doi:10.1080/10652460008819248

[78] Campos, L. M. B. C., "On the Extended Hypergeometric Equation and Functions of Arbitrary Degree," *Integral Transforms and Special Functions*, Vol. 11, No. 3, 2001, pp. 233–256. doi:10.1080/10652460108819315

[79] Campos, L. M. B. C., and Kobayashi, M. H. K., "On the Propagation of Sound in a High-Speed Non-Isothermal Shear Flow," *International Journal of Aeroacoustics*, Vol. 8, No. 3, 2009, pp. 199–230. doi:10.1260/147547208786940035

[80] Landau, L. D., and Lifshitz, E. F., *Fluid Mechanics*, Pergamon, New York, 1953.

[81] Kamke, E., *Differentialgleichungen*, Vol. 2, Chelsea Publ., American Mathematical Society, Providence, RI, 1972.

[82] Ronveaux, A. (ed.), *Heun's Differential Equation*, Oxford Univ. Press, New York, 1955.

C. Bailly
Associate Editor